

Thrust distribution in Higgs decays up to the fifth logarithmic order

Wan-Li Ju^{*}

INFN, Sezione di Milano, Via Celoria 16, 20133 Milano, Italy

Yongqi Xu[†]

*School of Physics and State Key Laboratory of Nuclear Physics and Technology,
Peking University, Beijing 100871, China*

Li Lin Yang[‡]

Zhejiang Institute of Modern Physics, School of Physics, Zhejiang University, Hangzhou 310027, China

Bin Zhou[§]

*INPAC, Shanghai Key Laboratory for Particle Physics and Cosmology, School of Physics and Astronomy,
Shanghai Jiao Tong University, Shanghai 200240, China*



(Received 19 May 2023; accepted 15 June 2023; published 28 June 2023)

In this work, we extend the resummation for the thrust distribution in Higgs decays up to the fifth logarithmic order. We show that one needs the accurate values of the three-loop soft functions for reliable predictions in the back-to-back region. This is especially true in the gluon channel, where the soft function exhibits poor perturbative convergence.

DOI: 10.1103/PhysRevD.107.114034

I. INTRODUCTION

The hadronic decays of the Higgs boson provide unique windows to study the Yukawa couplings of the lighter quarks such as the charm quark and the strange quark. These rare decays might be enhanced by new physics effects beyond the standard model (see, e.g., [1,2]) and can be probed at the Large Hadron Collider (LHC) and the future Higgs factories [3–7]. However, the hadronic decays of the Higgs boson can also proceed through the $H \rightarrow gg$ partonic channel. While the gluon channel is also useful, it is desirable to distinguish it from the $H \rightarrow q\bar{q}$ channel to gain maximal information about the Yukawa couplings. To this end, it is important to study various differential distributions in these two channels.

A classical differential distribution for hadronic final states is the event shape variable “thrust” [8]. It was extensively studied in the process $e^+e^- \rightarrow \text{hadrons}$. In the context of $H \rightarrow \text{hadrons}$, the next-to-leading order

(NLO) and approximate next-to-next-to-leading order (NNLO) predictions were calculated in [9]. These fixed-order results suffer from large logarithms in the endpoint region, which need to be resummed to all orders in the strong coupling α_s . The resummation framework is also well established for $e^+e^- \rightarrow \text{hadrons}$ [10–18]. The applications to the Higgs case were carried out in [19,20] at the next-to-next-to-leading logarithmic (NNLL and NNLL') accuracies. In this work, we extend the resummation accuracy up to the fifth order, and present the results at N³LL' and N⁴LL. Note that the logarithmic accuracies are affected by the availability of some coefficient functions and anomalous dimensions, as will be discussed in Sec. III.

The paper is organized as follows. In Sec. II we briefly review the factorization formula for the thrust distribution, and give technical details of the resummation framework. In Sec. III we provide numeric results for the resummed thrust distributions, with jet and soft scales chosen in the Laplace space. The summary and outlook come in Sec. IV. The alternative results with jet and soft scales chosen in the momentum space are presented in Appendix A, and we leave some lengthy expressions to the remaining appendices.

II. THEORETICAL FRAMEWORK

We consider the process $H \rightarrow \text{hadrons}$ induced by the following effective Lagrangian:

Published by the American Physical Society under the terms of the [Creative Commons Attribution 4.0 International license](#). Further distribution of this work must maintain attribution to the author(s) and the published article's title, journal citation, and DOI. Funded by SCOAP³.

$$\begin{aligned}\mathcal{L}_{\text{eff}} &= \frac{\alpha_s(\mu)C_t(m_t, \mu)}{12\pi v}O_g + \sum_q \frac{y_q(\mu)}{\sqrt{2}}O_q \\ &\equiv \frac{\alpha_s(\mu)C_t(m_t, \mu)}{12\pi v}HG^{\mu\nu,a}G_{\mu\nu}^a + \sum_q \frac{y_q(\mu)}{\sqrt{2}}H\bar{\psi}_q\psi_q,\end{aligned}\quad (1)$$

where v is the Higgs vacuum expectation value, H represents the physical Higgs boson after electroweak symmetry breaking, $G_{\mu\nu}^a$ is the field strength tensor of the gluon field, and ψ_q represent the light quark fields. We will ignore the masses of the light quarks but keep the Yukawa couplings y_q nonvanishing. The strong coupling α_s , the Yukawa coupling y_q , and the Wilson coefficient C_t

of the effective operator are renormalized in the $\overline{\text{MS}}$ scheme at the scale μ .

The thrust variable T is defined as

$$T \equiv \max_{\vec{n}} \frac{\sum_i |\vec{n} \cdot \vec{p}_i|}{\sum_i |\vec{p}_i|}, \quad (2)$$

where \vec{p}_i denote the 3-momenta of final state particles. The unit vector \vec{n} that maximize the above ratio is called the thrust axis. For convenience we introduce the variable $\tau \equiv 1 - T$. In this work we are concerned with the limit $T \rightarrow 1$ or $\tau \rightarrow 0$. Physically this corresponds to two back-to-back jets in the final state. In this limit the differential decay rate can be factorized into the product (convolution) of a hard function, a soft function, and two jet functions [9–12, 21–24]:

$$\begin{aligned}\frac{d\Gamma^q}{d\tau} &= \Gamma_B^q(\mu)|C_S^q(m_H, \mu)|^2 \int dp_n^2 dp_{\bar{n}}^2 dk \delta\left(\tau - \frac{p_n^2 + p_{\bar{n}}^2}{m_H^2} - \frac{k}{m_H}\right) J_n^q(p_n^2, \mu) J_{\bar{n}}^q(p_{\bar{n}}^2, \mu) S^q(k, \mu), \\ \frac{d\Gamma^g}{d\tau} &= \Gamma_B^g(\mu)|C_t(m_t, \mu)|^2 |C_S^g(m_H, \mu)|^2 \int dp_n^2 dp_{\bar{n}}^2 dk \delta\left(\tau - \frac{p_n^2 + p_{\bar{n}}^2}{m_H^2} - \frac{k}{m_H}\right) J_n^g(p_n^2, \mu) J_{\bar{n}}^g(p_{\bar{n}}^2, \mu) S^g(k, \mu),\end{aligned}\quad (3)$$

where the superscript q or g labels the partonic subprocesses $H \rightarrow q\bar{q}$ or $H \rightarrow gg$, with Γ_B^q and Γ_B^g being the corresponding total decay rates at the Born level. Their explicit expressions are

$$\Gamma_B^q = \frac{y_q^2(\mu)m_H C_A}{16\pi}, \quad \Gamma_B^g = \frac{\alpha_s^2(\mu)m_H^3}{72\pi^3 v^2}. \quad (4)$$

In the factorization formula, C_S^i (with $i = q, g$) are hard Wilson coefficients arising when matching the full theory of QCD to the soft-collinear effective theory (SCET) [25–30]; S^i are soft functions defined as the vacuum expectation values of soft Wilson-loop operators, J_n^i and $J_{\bar{n}}^i$ are jet functions along the two lightlike directions $n^\mu = (1, \vec{n})$, and $\bar{n}^\mu = (1, -\vec{n})$, where \vec{n} is the thrust axis.

The various ingredients satisfy renormalization group (RG) equations

$$\begin{aligned}\frac{d}{d \ln \mu} y_q(\mu) &= \gamma_y(\alpha_s(\mu)) y_q(\mu), \\ \frac{d}{d \ln \mu} C_t(m_t, \mu) &= \gamma_t(\alpha_s(\mu)) C_t(\mu^2), \\ \frac{d}{d \ln \mu} C_S^i(m_H, \mu) &= \left[\Gamma_{\text{cusp}}^i(\alpha_s(\mu)) \ln \frac{-m_H^2 - i\epsilon}{\mu^2} + \gamma_H^i(\alpha_s(\mu)) \right] C_S^i(m_H, \mu), \\ \frac{d}{d \ln \mu} J^i(p^2, \mu) &= \left[-2\Gamma_{\text{cusp}}^i(\alpha_s(\mu)) \ln \frac{p^2}{\mu^2} - 2\gamma_J^i(\alpha_s(\mu)) \right] J^i(p^2, \mu) + 2\Gamma_{\text{cusp}}^i(\alpha_s(\mu)) \int_0^{p^2} dq^2 \frac{J^i(p^2, \mu) - J^i(q^2, \mu)}{p^2 - q^2}, \\ \frac{d}{d \ln \mu} S^i(k, \mu) &= \left[4\Gamma_{\text{cusp}}^i(\alpha_s(\mu)) \ln \frac{k}{\mu} - 2\gamma_S^i(\alpha_s(\mu)) \right] S^i(k, \mu) - 4\Gamma_{\text{cusp}}^i(\alpha_s(\mu)) \int_0^k dq \frac{S^i(k, \mu) - S^i(q, \mu)}{k - q}.\end{aligned}\quad (5)$$

Note that the evolution equations for the jet and soft functions involve convolutions. It is useful to introduce the Laplace transformed functions

$$\begin{aligned}\tilde{j}^i(L_J, \mu) &= \int_0^\infty dp^2 \exp\left(-\frac{Np^2}{m_H^2}\right) J^i(p^2, \mu), \\ \tilde{s}^i(L_S, \mu) &= \int_0^\infty dk \exp\left(-\frac{Nk}{m_H}\right) S^i(k, \mu),\end{aligned}\quad (6)$$

where

$$L_J = \ln \frac{m_H^2}{\mu^2 \bar{N}}, \quad L_S = \ln \frac{m_H}{\mu \bar{N}}, \quad (7)$$

with $\bar{N} \equiv N e^{\gamma_E}$ and γ_E being the Euler's constant. The Laplace-space jet and soft functions satisfy local RG equations

$$\begin{aligned} \frac{d}{d \ln \mu} \tilde{j}^i(L_J, \mu) &= [-2\Gamma_{\text{cusp}}^i(\alpha_s(\mu))L_J - 2\gamma_J^i(\alpha_s(\mu))] \tilde{j}^i(L_J, \mu), \\ \frac{d}{d \ln \mu} \tilde{s}^i(L_S, \mu) &= [4\Gamma_{\text{cusp}}^i(\alpha_s(\mu))L_S - 2\gamma_S^i(\alpha_s(\mu))] \tilde{s}^i(L_S, \mu). \end{aligned} \quad (8)$$

Under the Laplace transform, the differential decay rates are expressed as

$$\begin{aligned} \int_0^\infty d\tau e^{-\tau N} \frac{d\Gamma^q}{d\tau} &= \Gamma_B^q(\mu) |C_S^q(m_H, \mu)|^2 [\tilde{j}^q(L_J, \mu)]^2 \tilde{s}^q(L_S, \mu), \\ \int_0^\infty d\tau e^{-\tau N} \frac{d\Gamma^g}{d\tau} &= \Gamma_B^g(\mu) |C_t(m_t, \mu)|^2 |C_S^g(m_H, \mu)|^2 \\ &\quad \times [\tilde{j}^g(L_J, \mu)]^2 \tilde{s}^g(L_S, \mu). \end{aligned} \quad (9)$$

For small τ , the dominant contribution arises from the region of large N . In this case the large logarithms L_J and L_S appear with increasing powers at each order in the perturbative expansions of the jet and soft functions. We will resum these logarithms to all orders in α_s using RG evolution.

In the RG equations, Γ_{cusp}^i are the cusp anomalous dimensions, which are known up to the four-loop accuracy [31–34], and their fifth-order contributions were estimated in [35]. The beta function governing the running strong coupling is known up to the five-loop order in [36–41]. The anomalous dimension γ^y for the Yukawa coupling is the same as that for the quark masses in the $\overline{\text{MS}}$ scheme, and is known up to the fifth order in [42–46]. The noncusp anomalous dimension γ_t governing scale evolution of the Wilson coefficient C_t is also known on the fifth level [47–52]. The up-to four-loop results for the remaining

TABLE I. Definitions of the logarithmic orders.

Logarithmic accuracy	$\Gamma_{\text{cusp}}, \beta$	$\gamma_{t,y,H,j,s}$	$C_t, C_S, \tilde{j}, \tilde{s}$
NNLL'	3-loop	2-loop	2-loop
$N^3\text{LL}$	4-loop	3-loop	2-loop
$N^3\text{LL}'$	4-loop	3-loop	3-loop
$N^4\text{LL}$	5-loop	4-loop	3-loop

anomalous dimensions can be found for γ_H^i in [53–62], for γ_S^i in [63–66], and for γ_J^i in [66–73]. The Wilson coefficient C_t is known up to the four-loop order [49–51, 74–77] and so is the hard sector [55, 57–62, 78] in the factorization of Eq. (3). As for the fixed-order expansions of the jet functions and the soft functions, the analytic results are known up to the three-loop order [11, 12, 67–73, 79, 80], with the exception of the scale-independent terms of the three-loop soft function. We collect all these ingredients in the Appendices B and C. They allow us to perform the resummation of large logarithms to the $N^3\text{LL}'$ order and approximately to the $N^4\text{LL}$ order. For the counting of logarithmic orders, we refer the reader to Table I.

To resum the large logarithms, we choose appropriate scales for each of the functions in the factorization formula, and use the RG equations to evolve them to a common scale. The choice of scales can be done either in the Laplace N -space or in the momentum τ -space. In the following, we present results with scale choices in the Laplace space, while those in the momentum space will be discussed in Appendix A. We choose the scales for the C_t , C_S , \tilde{j} , and \tilde{s} functions to be

$$\mu_t = e_t m_t, \quad \mu_h = e_h m_H, \quad \mu_j = e_j \frac{m_H}{\sqrt{N}}, \quad \mu_s = e_s \frac{m_H}{N}, \quad (10)$$

where by default we take $e_t = e_h = e_j = e_s = 1$, and we vary them up and down by a factor of 2 to estimate the associated uncertainties. The resummed differential decay rates in the Laplace space can be written as

$$\begin{aligned} \tilde{\Gamma}^q(N) &= \Gamma_B^q(\mu_h) U^q(\mu_h, \mu_j, \mu_s) |C_S^q(m_H, \mu_h)|^2 [\tilde{j}^q(L_J, \mu_j)]^2 \tilde{s}^q(L_S, \mu_s) \left(\frac{m_H}{\mu_s \bar{N}} \right)^{\eta_q}, \\ \tilde{\Gamma}^g(N) &= \Gamma_B^g(\mu_h) U^g(\mu_t, \mu_h, \mu_j, \mu_s) |C_t(m_t, \mu_t)|^2 |C_S^g(m_H, \mu_h)|^2 [\tilde{j}^g(L_J, \mu_j)]^2 \tilde{s}^g(L_S, \mu_s) \left(\frac{m_H}{\mu_s \bar{N}} \right)^{\eta_g}, \end{aligned} \quad (11)$$

where the evolution functions are given by

$$\begin{aligned} U^q(\mu_h, \mu_j, \mu_s) &= \exp \left[4S^q(\mu_h, \mu_j) + 4S^q(\mu_s, \mu_j) - 2A_{\text{cusp}}^q(\mu_h, \mu_j) \ln \frac{m_H^2}{\mu_h^2} - 2A_S^q(\mu_h, \mu_s) - 4A_J^q(\mu_h, \mu_j) \right], \\ U^g(\mu_t, \mu_h, \mu_j, \mu_s) &= \exp \left[2A_t(\mu_h, \mu_t) + 4S^g(\mu_h, \mu_j) + 4S^g(\mu_s, \mu_j) - 2A_{\text{cusp}}^g(\mu_h, \mu_j) \ln \frac{m_H^2}{\mu_h^2} - 2A_S^g(\mu_h, \mu_s) - 4A_J^g(\mu_h, \mu_j) \right], \end{aligned} \quad (12)$$

in which the functions $S^{q,g}$ and $A_i^{q,g}$ are defined by [81]

$$\begin{aligned} S^{q,g}(\nu, \mu) &= - \int_{\alpha_s(\nu)}^{\alpha_s(\mu)} d\alpha_s \frac{\Gamma_{\text{cusp}}^{q,g}(\alpha_s)}{\beta(\alpha_s)} \int_{\alpha_s(\nu)}^{\alpha_s} \frac{d\tilde{\alpha}_s}{\beta(\tilde{\alpha}_s)}, \\ A_i^{q,g}(\nu, \mu) &= - \int_{\alpha_s(\nu)}^{\alpha_s(\mu)} d\alpha_s \frac{\gamma_i^{q,g}(\alpha_s)}{\beta(\alpha_s)}, \end{aligned} \quad (13)$$

for $i = \text{cusp}, t, S, J$, and $\eta_{q,g} = 4A_{\text{cusp}}^{q,g}(\mu_j, \mu_s)$. The momentum-space differential decay rates can then be obtained through an inverse Laplace transform

$$\frac{d\Gamma^{q,g}}{d\tau} = \frac{1}{2\pi i} \int_{-i\infty}^{+i\infty} dN e^{N\tau} \tilde{\Gamma}^{q,g}(N). \quad (14)$$

The integration contour should, in principle, be chosen such that all singularities of the integrand are situated to the left side. However, the resummed integrand develops a Landau pole at large N due to the scale choices $\mu_j \sim m_H/\sqrt{N}$ and $\mu_s \sim m_H/\bar{N}$, which signals the breakdown of perturbation theory in that region. Correspondingly, the inverse Laplace transform of the perturbatively resummed integrand suffers from an ambiguity of nonperturbative origin. We adopt the so-called minimal prescription [82], in which the contour lies to the right of all physical singularities but to the left of the Landau pole.

With the generic framework, we still need to specify a few details in the evaluation of the resummed differential decay rates at a given logarithmic accuracy. The strong coupling α_s at a given scale μ is evaluated according to

$$\begin{aligned} \alpha_s(\mu) = & \frac{\alpha_s(\nu)}{X} \left\{ 1 - \frac{\alpha_s(\nu)\beta_1 \ln(X)}{4\pi X} + \left(\frac{\alpha_s(\nu)}{4\pi X} \right)^2 \left[\frac{\beta_1^2}{\beta_0^2} (\ln^2(X) - \ln(X) - 1 + X) + \frac{\beta_2}{\beta_0} (1 - X) \right] \right. \\ & + \left(\frac{\alpha_s(\nu)}{4\pi X} \right)^3 \left[\frac{\beta_1^3}{\beta_0^3} \left(-\frac{X^2}{2} + X - \ln^3(X) + \frac{5\ln^2(X)}{2} + 2(1-X)\ln(X) - \frac{1}{2} \right) + \frac{\beta_3}{2\beta_0} (1 - X^2) \right. \\ & + \frac{\beta_1\beta_2}{\beta_0^2} (2X\ln(X) - 3\ln(X) - X(1-X)) \Big] + \left(\frac{\alpha_s(\nu)}{4\pi X} \right)^4 \left[-\frac{\beta_4(X^3 - 1)}{3\beta_0} + \frac{\beta_3\beta_1}{6\beta_0^2} \right. \\ & \times ((X-1)(4X^2 + X + 1) + 6(X^2 - 2)\ln(X)) + \frac{\beta_2^2(X-1)^2(X+5)}{3\beta_0^2} + \frac{\beta_2\beta_1^2}{\beta_0^3} \\ & \times(-(X+3)(X-1)^2 + \ln(X)(-2X^2 + 5X - 3) - 3(X-2)\ln^2(X)) + \frac{\beta_1^4}{6\beta_0^4} \\ & \times ((X-1)^2(2X+7) + 6\ln^4(X) - 26\ln^3(X) + 9(2X-1)\ln^2(X) + 6(X-4)(X-1)\ln(X)) \Big] \Big\}, \end{aligned} \quad (15)$$

where the initial scale is chosen at the Z boson mass, $\nu = m_Z$, and

$$X = 1 + \frac{\alpha_s(\nu)}{2\pi} \beta_0 \ln \frac{\mu}{m_Z}. \quad (16)$$

The coefficients of the beta function are defined through

$$\frac{d\alpha_s}{d \ln \mu} = -2\alpha_s \sum_{n=0}^{\infty} \left(\frac{\alpha_s}{4\pi} \right)^{n+1} \beta_n. \quad (17)$$

The Yukawa coupling y_q at a given scale is evaluated with

$$y_q(\mu) = y_q(m_H) \exp[A_y^q(\mu, m_H)]. \quad (18)$$

The evolution factors $U^{q,g}$ and the factors involving $\eta_{q,g}$ are expanded on the exponent up to a given logarithmic accuracy defined in Table I. The expansion is done by counting the large logarithms $\ln(\nu/\mu)$ as $\mathcal{O}(1/\alpha_s)$. The

fixed-order factors ($|C_S^q|^2 |\tilde{j}^q|^2 \tilde{s}^q$ and $|C_t|^2 |C_S^g|^2 |\tilde{j}^g|^2 \tilde{s}^g$) are also expanded up to a given loop order. We are now ready to perform numeric evaluations of the resummed differential decay rates. The results are presented in the next section.

III. NUMERIC RESULTS

A. Choice of parameters and estimation of uncertainties

In this section we are devoted to the numeric results. Throughout this paper, we choose $\alpha_s(m_Z) = 0.1181$, $m_H = 125.1$ GeV, and $m_t = 172.9$ GeV [83]. The scales are chosen as in Eq. (10). Note that this choice is conventional in the small- τ region considered in this work. On the other hand, if one wants to match the resummed distributions to the fixed-order ones, it is necessary to deal with the intermediate regime between the resummation dominated small- τ region and the fixed-order dominated large- τ region. We leave this subtlety to future investigations.

We estimate the perturbative uncertainties by varying each of e_t , e_h , e_j , and e_s up and down by a factor of 2, while keeping the others at their defaults. The resulting variations of the differential decay rates are then added in quadrature.

The scale-independent constant terms of the three-loop soft functions are not known yet. The term in the quark channel was extracted in [71] through a numeric fit to the fixed-order thrust distribution, which has a large uncertainty. In this work we set

$$c_{3g}^S = -19988 \pm 5000, \quad (19)$$

and estimate the corresponding variation of the resummed distribution. For the gluon channel we apply the Casimir scaling and set

$$c_{3g}^S = -45433 \pm 11250. \quad (20)$$

The five-loop cusp anomalous dimensions are also unknown, with only a rough estimation available [35]. However, we have checked that they only have a rather mild effect on the resummed thrust distributions.

B. The resummed thrust distributions in the gluon channel

We now show the resummed thrust distributions in the gluon channel at various logarithmic accuracies. The baseline for comparison is the NNLL' result, that is the state-of-the-art accuracy in the literature (see Refs. [19,20], although they adopted scale choices in the momentum space).

In Fig. 1, we show the comparison between NNLL' and N³LL, and that between NNLL' and N³LL', for the τ range [0.01, 0.15]. This covers the small- τ and intermediate- τ regions, but cuts out the large- τ region where fixed-order matching would be important. One can see that the N³LL result has a slightly reduced scale uncertainty compared to

the NNLL' one. The reduction is most significant in the small- τ region, where resummation effects are expected to be important. The N³LL' result further reduces the scale uncertainty in the intermediate τ region, with the three-loop hard, jet and soft functions included. However, we observe an unusual increase of scale uncertainty in the small τ region, as is clear from the right plot of Fig. 1. It can be seen that the two bands even do not overlap below $\tau \sim 0.03$. This fact can be traced to the unusually large constant term c_{3g}^S of the three-loop soft function. It is instructive to show the soft function at its default scale $\mu_s = m_H/\bar{N}$, where $L_S = 0$, for $c_{3g}^S = -45433$:

$$\begin{aligned} \tilde{s}^g(0, \mu_s) &= 1 - 2.356\alpha_s(\mu_s) + 1.617\alpha_s^2(\mu_s) \\ &\quad - 22.90\alpha_s^3(\mu_s) + \dots \end{aligned} \quad (21)$$

For small τ , one expects that the dominant contributions in the Laplace space come from the region where $\tau N \sim 1$. This means that, below $\tau \sim 0.03$, μ_s is typically only about a few GeVs, where $\alpha_s \sim 0.2$ is not so small. Therefore, the gluon soft function has a rather poor perturbative convergence if we take the fitted central value of c_{3g}^S . It is highly desired to calculate the exact value of c_{3g}^S to settle down this issue: either its absolute value is in fact smaller, and the N³LL' result is already sufficient, or it is indeed that large, then one needs to have even higher order corrections for reliable predictions. Efforts towards this goal are being actively pursued in the literature [84,85].

To demonstrate the effects of different values of c_{3g}^S , we show in the left plot of Fig. 2 the resummed distributions for three values of c_{3g}^S : the default value -45433 , the “lower” value -56683 , and the “upper” value -34183 . Note that since the fitted value of c_{3g}^S is negative, the “upper” value has a smaller absolute value, and leads to a better perturbative convergence. Indeed, as can be seen

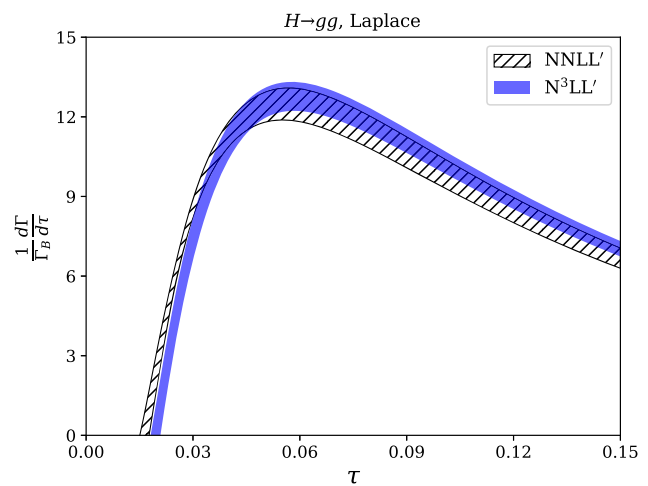
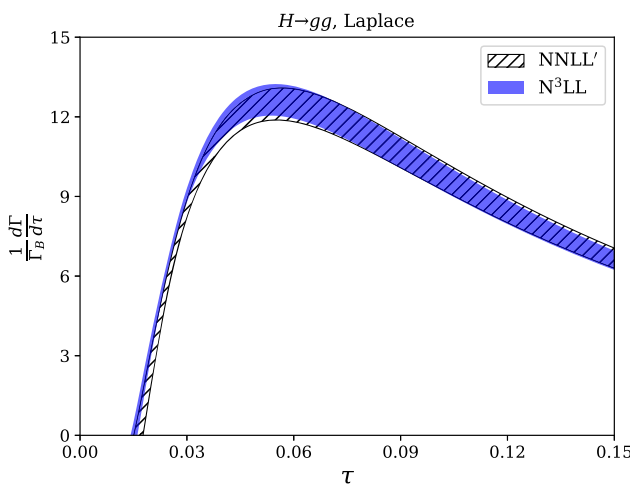


FIG. 1. The resummed thrust distributions in the gluon channel. Left: NNLL' vs N³LL. Right: NNLL' vs N³LL'.

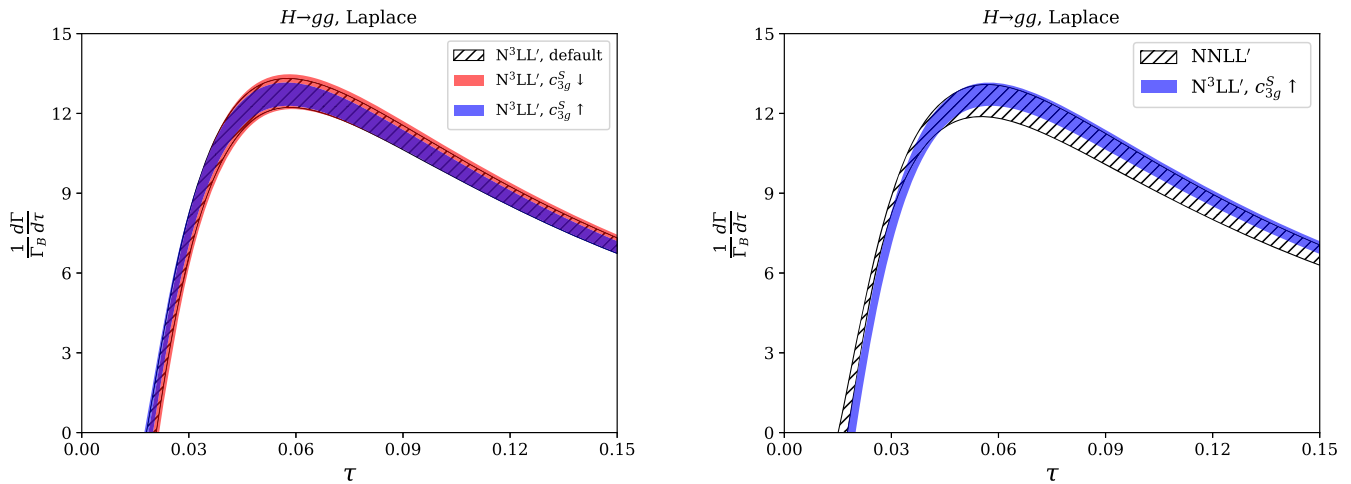


FIG. 2. The effects of c_{3g}^S on the N^3LL' results in the gluon channel. Left: N^3LL' results with three values of c_{3g}^S . Right: $NNLL'$ vs N^3LL' where c_{3g}^S is taken to its “upper” value (with a smaller absolute value).

from the plot, the result with the “upper” value exhibits a smaller scale uncertainty, especially in the small- τ region. It is also evident from the right plot of Fig. 2, that the N^3LL' band is better overlapped with the $NNLL'$ one with c_{3g}^S taking the “upper” value. Finally for reference, we list in Table II the variations of the N^3LL' differential decay rate at $\tau = 0.05$ induced by changing the values of various scales as well as c_{3g}^S . It is clear that the main source of the scale uncertainty comes from the soft scale, as expected. It can also be seen that varying c_{3g}^S has a larger effect than varying μ_t , μ_h , or μ_j . All these emphasize again that we need a better understanding of the soft function at and beyond three loops.

It is tempting to combine the uncertainties due to c_{3g}^S with the scale uncertainties in quadrature. We have done this exercise and show the results in Fig. 3. We find that the additional variation from c_{3g}^S has only a small effect when combined in this way. We emphasize again that the main impacts of c_{3g}^S are the large corrections at small τ as observed in Fig. 1, and the different sizes of scale variations with different values of c_{3g}^S as observed in Fig. 2.

We now add another layer of resummation on top of N^3LL' , and present the results at N^4LL . The results are shown in Fig. 4, with explicit numbers at $\tau = 0.05$ given in Table III. We find that the additional order of resummation has a mild effect on the distribution, that is only clearly

visible in the peak region. It is also evident that the five-loop cusp anomalous dimension does not have important impacts.

C. The resummed thrust distributions in the quark-antiquark channel

We now briefly discuss the results in the quark-antiquark channel. In the left plot of Fig. 5, we compare the $NNLL'$ result against the N^3LL' one, where the three-loop constant term c_{3g}^S of the soft function is chosen at the default value. We again observe that the uncertainty band of N^3LL' is broader than the $NNLL'$ one, especially at the lower end of the distribution. In the right plot of Fig. 5, we show the N^3LL' distributions for three values of c_{3g}^S : the default value -19988 , the “upper” value -14988 , and the “lower” value

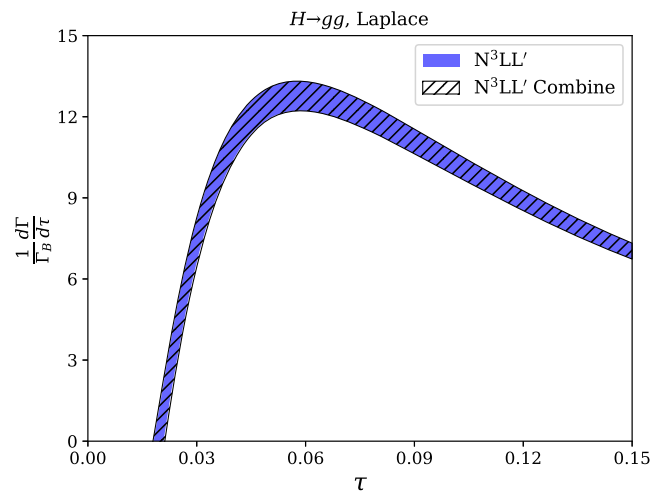


TABLE II. Variations of the N^3LL' differential decay rate at $\tau = 0.05$ induced by changing the scales and c_{3g}^S . The central value is 12.120.

$H \rightarrow gg, N^3LL'$	μ_t	μ_h	μ_j	μ_s	c_{3g}^S
Max	12.128	12.120	12.120	13.077	12.219
Min	12.106	11.967	12.063	12.044	12.020

FIG. 3. The effect of combining the variation due to c_{3g}^S into the total uncertainties.

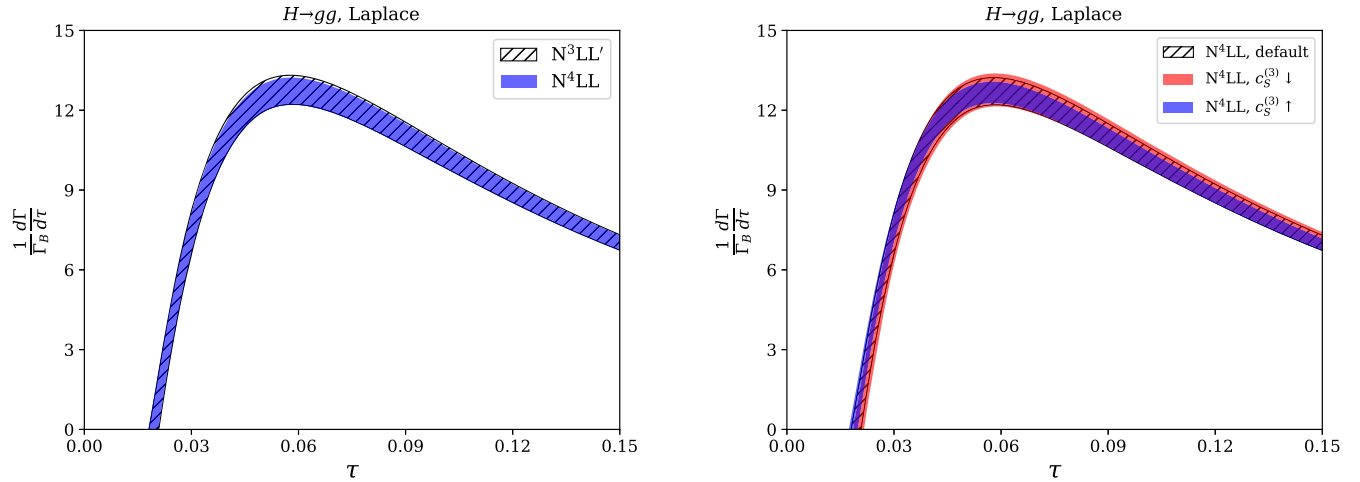


FIG. 4. The resummed thrust distributions in the gluon channel. Left: N^3LL' vs N^4LL . Right: N^4LL results with three values of c_{3q}^S .

TABLE III. Variations of the N^4LL differential decay rate at $\tau = 0.05$ induced by changing the scales, c_{3q}^S and the five-loop cusp anomalous dimension $\Gamma_{\text{cusp}}^{g(4)}$. The central value is 12.084.

$H \rightarrow gg, N^4LL$	μ_t	μ_h	μ_j	μ_s	c_{3q}^S	$\Gamma_{\text{cusp}}^{g(4)}$
Max	12.089	12.084	12.084	12.980	12.183	12.085
Min	12.073	11.936	12.025	12.022	11.985	12.083

-24988. As expected, the band becomes narrower for the “upper” value, where the absolute value of c_{3q}^S is smaller, and the soft function has a perturbative convergence. Overall, the uncertainties of the resummed thrust distributions in the $q\bar{q}$ channel are significantly smaller than those in the gluon channel. This can be partly explained by the smaller color factor C_F compared to C_A .

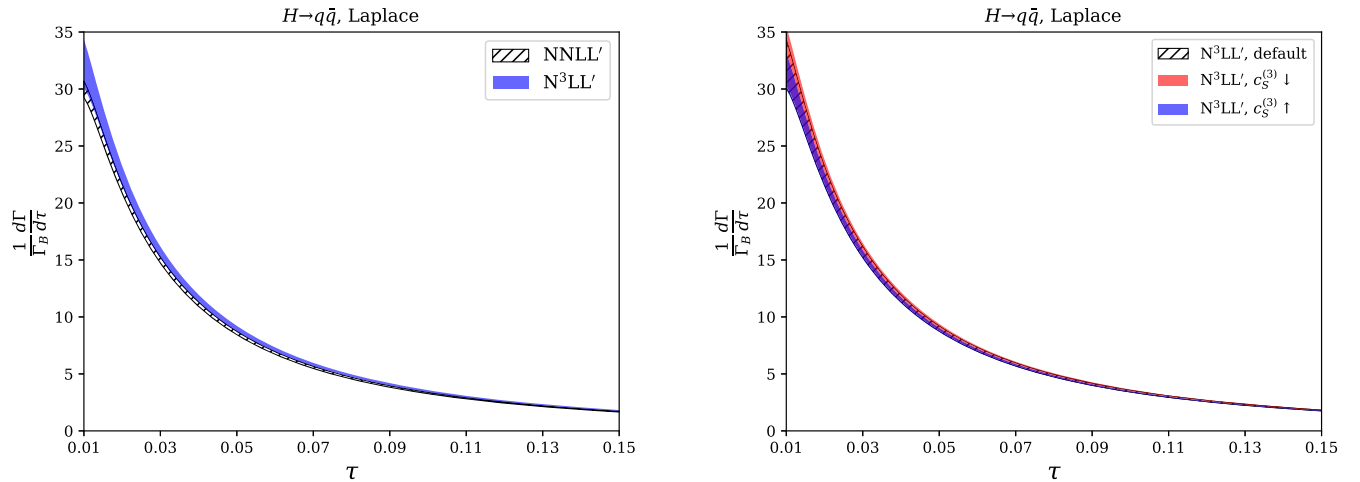


FIG. 5. The resummed thrust distributions in the $q\bar{q}$ channel. Left: $NNLL'$ vs N^3LL' . Right: N^3LL' results with three values of c_{3q}^S .

IV. SUMMARY AND OUTLOOK

In this work, we extend the resummation for the thrust distribution in Higgs decays up to the fifth logarithmic order. A main conclusion that can be drawn from our results is that one needs the accurate values of the three-loop soft functions for reliable predictions in the small- τ region. This is especially true in the gluon channel, where the perturbative convergence of the soft function seems to be rather bad with a large three-loop constant term.

Once the three-loop soft functions become available, the ingredients collected in this work will allow for faithful numeric predictions at the N^3LL' and N^4LL accuracies. Depending on the size of the three-loop constant, it is possible that one even needs the four-loop gluon soft function to reduce the scale uncertainties and obtain reliable predictions in the small- τ region.

Finally, given the high logarithmic accuracy at leading power achieved in this work, it is also necessary and interesting to include the subleading power contributions [86,87]. On one hand, the numeric impacts of the subleading terms are comparable to the N^3LL' corrections in the peak region. On the other hand, the subleading terms are extremely important in the intermediate- τ region, when matching the resummed distributions to the fixed-order ones. We leave these to future investigations.

ACKNOWLEDGMENTS

This work was supported in part by the National Natural Science Foundation of China under Grants No. 11975030 and No. 12147103, and the Fundamental Research Funds for the Central Universities.

APPENDIX A: CHOICE OF SCALES IN THE MOMENTUM SPACE

In the main text, we have chosen the jet and soft scales in the Laplace space, and performed the inverse Laplace transform numerically. A different approach is to set the jet and soft scales independent of the Laplace variable N . In this case, the inverse Laplace transform (14) can be carried out analytically [12,81,88]. For simplicity we only discuss the gluon channel in this appendix. The result can be written as

$$\begin{aligned} \frac{d\Gamma^g}{d\tau} = & \Gamma_B^g(\mu_h) U^g(\mu_t, \mu_h, \mu_j, \mu_s) |C_t(m_t, \mu_t)|^2 |C_S^g(m_H, \mu_h)|^2 \\ & \times \left[\tilde{j}^g \left(\ln \frac{\mu_s m_H}{\mu_j^2} + \partial_{\eta_g}, \mu_s \right) \right]^2 \tilde{s}^g(\partial_{\eta_g}, \mu_s) \\ & \times \left[\frac{1}{\tau \Gamma(\eta_g)} \left(\frac{\tau m_H}{\mu_s e^{\gamma_E}} \right)^{\eta_g} \right]. \end{aligned} \quad (\text{A1})$$

The common practice is then to choose μ_s and μ_j as a function of τ , such that $\mu_j \sim \sqrt{\tau m_H}$ and $\mu_s \sim \tau m_H$ in the small- τ region. In this work we do not care about matching with the fixed-order results in the large- τ region (otherwise one needs to introduce “profile scales” as in [19,20]). Therefore we can adopt the simplest choices

$$\mu_t = e_t m_t, \quad \mu_h = e_h m_H, \quad \mu_j = e_j \sqrt{\tau m_H}, \quad \mu_s = e_s \tau m_H, \quad (\text{A2})$$

where the parameters e_t , e_h , e_j , and e_s are set to 1 by default, and are varied up and down by a factor of 2 to estimate the uncertainties. The numeric results with the above scale choices are shown in Fig. 6. We observe very large scale uncertainties in the small- τ region, much larger than those seen in Fig. 1. As it turns out, these large uncertainties originate from the jet and soft scales, i.e., e_j and e_s .

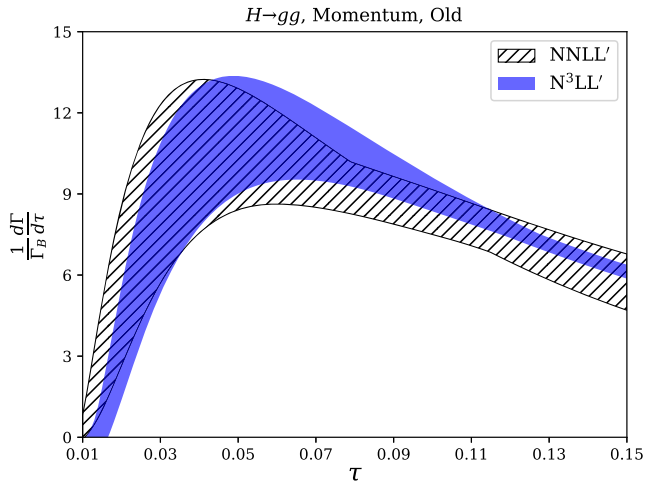


FIG. 6. The resummed thrust distributions at NNLL' and N^3LL' in the gluon channel with the scale choices (A2) at the level of differential decay rates.

The prescription in Eq. (A2) actually has a subtle problem related exactly to the jet and soft scales. The formula (A1) is based on the solutions to the RG equations (5). Taking the gluon jet function as an example, the RG equation is

$$\begin{aligned} \frac{d}{d \ln \mu} J^g(p^2, \mu) = & \left[-2\Gamma_{\text{cusp}}^g(\alpha_s(\mu)) \ln \frac{p^2}{\mu^2} - 2\gamma_J^g(\alpha_s(\mu)) \right] J^g(p^2, \mu) \\ & + 2\Gamma_{\text{cusp}}^g(\alpha_s(\mu)) \int_0^{p^2} dq^2 \frac{J^g(p^2, \mu) - J^g(q^2, \mu)}{p^2 - q^2}. \end{aligned} \quad (\text{A3})$$

And the solution reads [81,88]

$$\begin{aligned} J^g(p^2, \mu) = & \exp [-4S^g(\mu_j, \mu) + 2A_J^g(\mu_j, \mu)] \tilde{j}^g(\partial_\eta, \mu_j) \\ & \times \left[\frac{1}{p^2} \left(\frac{p^2}{\mu_j^2} \right)^\eta \right]_* \frac{e^{-\gamma_E \eta}}{\Gamma(\eta)}, \end{aligned} \quad (\text{A4})$$

where $\eta = 2A_{\text{cusp}}^g(\mu_j, \mu)$, and the star distribution is defined by

$$\begin{aligned} \int_0^{Q^2} dp^2 \left[\frac{1}{p^2} \left(\frac{p^2}{\mu_j^2} \right)^\eta \right]_* f(p^2) = & \int_0^{Q^2} dp^2 \frac{f(p^2) - f(0)}{p^2} \left(\frac{p^2}{\mu_j^2} \right)^\eta \\ & + \frac{f(0)}{\eta} \left(\frac{Q^2}{\mu^2} \right)^\eta. \end{aligned} \quad (\text{A5})$$

The solution is of course formally independent of μ_j . However, at any finite order there is a residue dependence. Assuming that μ_j is independent of p^2 , the above solution indeed satisfies the RG equation (A3), where μ_j is the same in both $J^g(p^2, \mu)$ and $J^g(q^2, \mu)$. However, the scale choice

in Eq. (A2) actually makes μ_j correlated with $p^2 \sim \tau m_H^2$. That is, $\mu_j^2 \sim p^2$ in $J^g(p^2, \mu)$ and $\mu_j^2 \sim q^2$ in $J^g(q^2, \mu)$. This immediately renders the convolution in Eq. (A3) ill defined due to the singularity as $q^2 \rightarrow 0$.

One may of course ignore the problem with Eq. (A3) and insist on using Eq. (A4) with $\mu_j \sim p^2$ as the resummed jet function. As long as one does not take $p^2 \rightarrow 0$ (where

nonperturbative physics enters anyway), this does not pose any difficulty at face value. However, let us take a closer look. We set $\mu_j = e_j \sqrt{p^2}$ in Eq. (A4), and truncate the solution at NLL' accuracy (that means two-loop Γ_{cusp}^g , one-loop γ_j^g , and one-loop \tilde{j}^g). We then expand the resummed jet function in terms of $\alpha_s(\mu)$. This gives

$$\begin{aligned} J^{g,\text{NLL}'}(p^2, \mu; \mu_j = e_j \sqrt{p^2}) &= \frac{\alpha_s(\mu)}{4\pi} \frac{1}{p^2} \left(12 \ln \frac{p^2}{\mu^2} - \frac{23}{3} \right) + \left(\frac{\alpha_s(\mu)}{4\pi} \right)^2 \frac{1}{p^2} \\ &\times \left[576 \ln^3(e_j) + 736 \ln^2(e_j) + \left(\frac{9364}{9} - 144\pi^2 \right) \ln(e_j) + 72 \ln^3 \left(\frac{p^2}{\mu^2} \right) + \dots \right] + \mathcal{O}(\alpha_s^3), \end{aligned} \quad (\text{A6})$$

where the ellipsis denotes further e_j -independent terms. We can see that the e_j dependence cancels at order α_s^1 , as it should at the NLL' accuracy. However, there exist rather high powers of $\ln(e_j)$ at order α_s^2 (and beyond). While $\ln(e_j)$ is counted as a “small” logarithm, these high powers lead to large uncertainties of the resummed jet function when e_j is varied between 1/2 and 2. The resummed soft function $S^g(k, \mu)$ with $\mu_s = e_s k$ exhibits similar behavior. These explain the large uncertainty bands observed in Fig. 6. In practice, it is often argued that e_j and e_s are not independent and should be correlated. This can result in partial cancellations between the $\ln^n(e_j)$ and $\ln^n(e_s)$ terms, and lead to smaller uncertainty estimations.

$$J^{g,\text{NLL}'}(p^2, \mu; \mu_j = e_j m_H / \sqrt{\bar{N}}) = \frac{\alpha_s(\mu)}{4\pi} \frac{1}{p^2} \left(12 \ln \frac{p^2}{\mu^2} - \frac{23}{3} \right) + \left(\frac{\alpha_s(\mu)}{4\pi} \right)^2 \frac{1}{p^2} \left[72 \ln^3 \left(\frac{p^2}{\mu^2} \right) + \dots \right] + \mathcal{O}(\alpha_s^3). \quad (\text{A8})$$

Evidently, all the $\ln^n(e_j)$ terms drop out at order α_s^2 . This explains the smaller uncertainty bands in Fig. 1 compared to Fig. 6.

There is an alternative way of choosing the jet and soft scales in the momentum space [18,89,90]. We define the accumulative decay rate as

$$\hat{\Gamma}^g(\tau) \equiv \int_0^\tau \frac{d\Gamma^g}{d\tau'} d\tau'. \quad (\text{A9})$$

In the above integrals, μ_j and μ_s are set to the same expressions as in Eq. (A2), where τ is the upper bound of the integration. The jet and soft scales are hence independent of the integration variable τ' . Before resummation, the factorization formula for the accumulative decay rates can be obtained by integrating Eq. (3) over τ . The result reads

The above behavior does not occur with the scale choices in Eq. (10). We can do the same exercise with $\mu_j = e_j m_H / \sqrt{\bar{N}}$ in the Laplace space. The resummed Laplace-space jet function is given by

$$\begin{aligned} \tilde{j}^g(L_J, \mu) &= \exp [-4S^g(\mu_j, \mu) + 2A_J^g(\mu_j, \mu)] \\ &\times \left(\frac{m_H^2}{\bar{N}\mu_j^2} \right)^\eta \tilde{j}^g(L_J, \mu_j). \end{aligned} \quad (\text{A7})$$

Again truncating at the NLL' accuracy and expanding in terms of $\alpha_s(\mu)$, we can perform the inverse Laplace transform analytically to arrive at

$$\begin{aligned} \hat{\Gamma}^g(\tau) &= \Gamma_B^g(\mu) |C_t(m_t, \mu)|^2 |C_S^g(m_H, \mu)|^2 \\ &\times \int dp_n^2 dp_{\bar{n}}^2 dk \hat{j}_n^g(p_n^2, \mu) \hat{j}_{\bar{n}}^g(p_{\bar{n}}^2, \mu) S^g(k, \mu), \end{aligned} \quad (\text{A10})$$

where the integration domain is determined by the constraints

$$\tau \geq \frac{p_n^2 + p_{\bar{n}}^2}{m_H^2} + \frac{k}{m_H}, \quad p_n^2, p_{\bar{n}}^2, k \geq 0. \quad (\text{A11})$$

Now, since the jet scale μ_j is a function of τ and is independent of p^2 , the problem with the convolution in Eq. (A3) is absent here.

After resummation, the accumulative decay rate is

$$\begin{aligned} \hat{\Gamma}^g(\tau) &= \Gamma_B^g(\mu_h) U^g(\mu_t, \mu_h, \mu_j, \mu_s) |C_t(m_t, \mu_t)|^2 |C_S^g(m_H, \mu_h)|^2 \\ &\times \left[\tilde{j}^g \left(\ln \frac{\mu_s m_H}{\mu_j^2} + \partial_{\eta_g}, \mu_j \right) \right]^2 \tilde{s}^g(\partial_{\eta_g}, \mu_s) \\ &\times \left[\frac{1}{\Gamma(1 + \eta_g)} \left(\frac{\tau m_H}{\mu_s e^{\gamma_E}} \right)^{\eta_g} \right]. \end{aligned} \quad (\text{A12})$$

We set the jet and soft scales at the accumulative level following Eq. (A2), i.e., $\mu_j = e_j \sqrt{\tau m_H}$ and $\mu_s = e_s \tau m_H$. We then take the derivative with respect to τ to obtain the resummed differential decay rate:

$$\frac{d\Gamma^g}{d\tau} = \frac{d}{d\tau} \hat{\Gamma}^g(\tau). \quad (\text{A13})$$

The numeric results with this new prescription are plotted in Fig. 7.

To compare the “new” way of scale setting at the accumulative level with the “old” way at the differential level, we can study the resummed integrated jet function

$$\begin{aligned} \hat{J}^g(p^2, \mu) &= \int_0^{p^2} dq^2 J^g(q^2, \mu) \\ &= \exp[-4S^g(\mu_j, \mu) + 2A_J^g(\mu_j, \mu)] \\ &\times \tilde{j}^g(\partial_\eta, \mu_j) \left(\frac{p^2}{\mu_j^2} \right)^\eta \frac{e^{-\gamma_E \eta}}{\Gamma(1 + \eta)}, \end{aligned} \quad (\text{A14})$$

with $\mu_j = e_j \sqrt{p^2}$. This is part of the resummed accumulative decay rate (A12). We still truncate at the NLL’ accuracy and expand in terms of $\alpha_s(\mu)$. We then take the derivative with respect to p^2 and arrive at

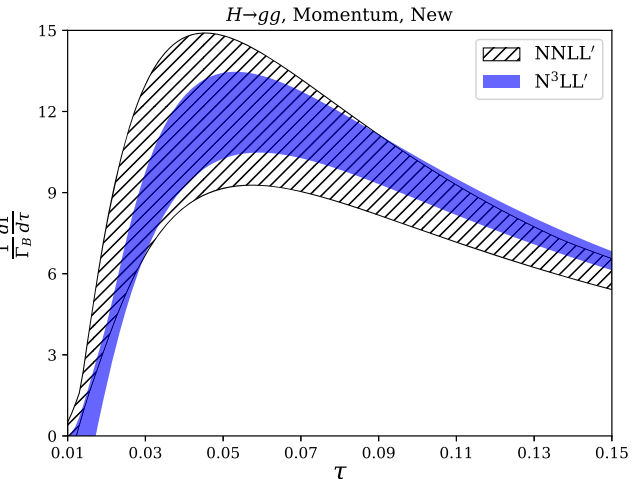


FIG. 7. The resummed thrust distributions at NNLL’ and N^3LL' in the gluon channel with the scale choices (A2) at the level of accumulative decay rates.

$$\begin{aligned} &\frac{\partial}{\partial p^2} \hat{j}^{g,\text{NNLL}'}(p^2, \mu; \mu_j = e_j \sqrt{p^2}) \\ &= \frac{\alpha_s(\mu)}{4\pi} \frac{1}{p^2} \left(12 \ln \frac{p^2}{\mu^2} - \frac{23}{3} \right) \\ &+ \left(\frac{\alpha_s(\mu)}{4\pi} \right)^2 \frac{1}{p^2} \left[72 \ln^3 \left(\frac{p^2}{\mu^2} \right) + \dots \right] + \mathcal{O}(\alpha_s^3). \end{aligned} \quad (\text{A15})$$

We see that the order α_s^2 term is indeed independent of e_j .

APPENDIX B: FIXED ORDER INGREDIENTS

In this appendix we list the fixed-order ingredients appearing in the resummation formula (11).

The Wilson coefficient C_t is known up to the four-loop order [47–52]. For our purpose, we need its expression up to three loops, which is given by

$$\begin{aligned} C_t(m_t, \mu) &= 1 + \frac{\alpha_s}{4\pi} 11 + \left(\frac{\alpha_s}{4\pi} \right)^2 \left[L_t \left(19 + \frac{16}{3} n_f \right) + \frac{2777}{18} - \frac{67}{6} n_f \right] + \left(\frac{\alpha_s}{4\pi} \right)^3 \left[L_t^2 \left(209 + 46n_f - \frac{32}{9} n_f^2 \right) \right. \\ &+ L_t \left(\frac{4834}{9} + \frac{2912}{27} n_f + \frac{77}{27} n_f^2 \right) - \frac{2761331}{648} + \frac{897943\zeta_3}{144} + \left(\frac{58723}{324} - \frac{110779\zeta_3}{216} \right) n_f - \frac{6865}{486} n_f^2 \Big], \end{aligned} \quad (\text{B1})$$

where $L_t = \ln(\mu^2/m_t^2)$, and we have explicitly set the number of colors $N_c = 3$ to shorten the expression.

The hard Wilson coefficients $C_S^{q,g}$ are expanded as

$$C_S^{q,g}(m_H, \mu) = \sum_{n=0} \left(\frac{\alpha_s}{4\pi} \right)^n C_S^{q,g(n)}, \quad (\text{B2})$$

where the gluon channel coefficients up to three-loop order are given by [59]

$$\begin{aligned}
C_S^{g(0)} &= 1, \\
C_S^{g(1)} &= \left(\frac{\pi^2}{6} - L^2\right) C_A, \\
C_S^{g(2)} &= n_f C_A \left[-\frac{2L^3}{9} + \frac{10L^2}{9} + \left(\frac{52}{27} + \frac{2\pi^2}{9}\right)L - \frac{46\zeta_3}{9} - \frac{5\pi^2}{18} - \frac{916}{81} \right] \\
&\quad + C_A^2 \left[\frac{L^4}{2} + \frac{11L^3}{9} + \left(\frac{\pi^2}{6} - \frac{67}{9}\right)L^2 + L \left(-2\zeta_3 - \frac{11\pi^2}{9} + \frac{80}{27}\right) - \frac{143\zeta_3}{9} \right. \\
&\quad \left. + \frac{\pi^4}{72} + \frac{67\pi^2}{36} + \frac{5105}{162} \right] + n_f C_F \left(2L + 8\zeta_3 - \frac{67}{6} \right), \\
C_S^{g(3)} &= n_f C_A C_F \left[-\frac{8L^3}{3} + L^2(13 - 16\zeta_3) + L \left(-\frac{376\zeta_3}{9} + \frac{4\pi^4}{45} + \pi^2 + \frac{3833}{54}\right) \right. \\
&\quad \left. + \frac{32\pi^2\zeta_3}{9} + \frac{14564\zeta_3}{81} + \frac{608\zeta_5}{9} - \frac{34\pi^2}{27} - \frac{16\pi^4}{405} - \frac{341219}{972} \right] \\
&\quad + n_f^2 C_A \left[-\frac{2L^4}{27} + \frac{40L^3}{81} + \left(\frac{116}{81} + \frac{4\pi^2}{27}\right)L^2 + L \left(-\frac{128\zeta_3}{27} - \frac{40\pi^2}{81} - \frac{14057}{729}\right) \right. \\
&\quad \left. + \frac{4576\zeta_3}{243} + \frac{\pi^4}{243} + \frac{2\pi^2}{27} + \frac{611401}{13122} \right] + n_f C_A^2 \left[\frac{2L^5}{9} - \frac{8L^4}{27} + \left(-\frac{734}{81} - \frac{\pi^2}{9}\right)L^3 \right. \\
&\quad \left. + L^2 \left(\frac{118\zeta_3}{9} + \frac{377}{27} - \frac{103\pi^2}{54}\right) + L \left(\frac{28\zeta_3}{9} + \frac{1910\pi^2}{243} - \frac{4\pi^4}{15} + \frac{133036}{729}\right) + \frac{428\zeta_5}{9} \right. \\
&\quad \left. - \frac{41\pi^2\zeta_3}{27} - \frac{460\zeta_3}{81} + \frac{73\pi^4}{1620} - \frac{14189\pi^2}{4374} - \frac{3765007}{6561} \right] + C_A^3 \left[-\frac{L^6}{6} - \frac{11L^5}{9} \right. \\
&\quad \left. + \left(\frac{281}{54} - \frac{\pi^2}{4}\right)L^4 + L^3 \left(2\zeta_3 + \frac{11\pi^2}{18} + \frac{1540}{81}\right) + L^2 \left(\frac{143\zeta_3}{9} + \frac{685\pi^2}{108} - \frac{6740}{81} - \frac{73\pi^4}{360}\right) \right. \\
&\quad \left. + L \left(\frac{17\pi^2\zeta_3}{9} + \frac{2048\zeta_3}{27} + 16\zeta_5 + \frac{44\pi^4}{45} - \frac{6710\pi^2}{243} - \frac{373975}{1458}\right) + \frac{2222\zeta_5}{9} \right. \\
&\quad \left. - \frac{104\zeta_3^2}{9} - \frac{605\pi^2\zeta_3}{54} - \frac{152716\zeta_3}{243} + \frac{105617\pi^2}{4374} - \frac{1939\pi^4}{9720} + \frac{29639273}{26244} - \frac{24389\pi^6}{408240} \right] \\
&\quad + n_f^2 C_F \left[\frac{4L^2}{3} + L \left(\frac{32\zeta_3}{3} - \frac{52}{3}\right) - \frac{112\zeta_3}{3} - \frac{10\pi^2}{27} + \frac{4481}{81} - \frac{4\pi^4}{405} \right] \\
&\quad + n_f C_F^2 \left[-2L + \frac{296\zeta_3}{3} - 160\zeta_5 + \frac{304}{9} \right], \tag{B3}
\end{aligned}$$

and the quark channel coefficients are given by [60]

$$\begin{aligned}
C_S^{q(0)} &= 1, \\
C_S^{q(1)} &= \frac{1}{6}(-6L^2 + \pi^2 - 12)C_F, \\
C_S^{q(2)} &= C_F^2 \left[\frac{L^4}{2} + \left(2 - \frac{\pi^2}{6}\right)L^2 + 6(4L - 5)\zeta_3 - 2\pi^2 L + \frac{7\pi^2}{3} - \frac{83\pi^4}{360} + 6 \right] \\
&\quad + C_F \left[\frac{11L^3 C_A}{9} + \frac{1}{3}\pi^2 L^2 C_A - \frac{67L^2 C_A}{9} - 26L\zeta_3 C_A + \frac{11}{9}\pi^2 L C_A + \frac{242LC_A}{27} \right. \\
&\quad \left. + \frac{151\zeta_3 C_A}{9} + \frac{11\pi^4 C_A}{45} - \frac{467C_A}{81} - \frac{103\pi^2 C_A}{108} - \frac{10L^3}{9} + \frac{50L^2}{9} - \frac{10\pi^2 L}{9} - \frac{280L}{27} + \frac{10\zeta_3}{9} + \frac{25\pi^2}{54} + \frac{1000}{81} \right],
\end{aligned}$$

$$\begin{aligned}
C_S^{q(3)} = & C_F^3 \left[-\frac{L^6}{6} + \frac{\pi^2 L^4}{12} - L^4 - 24L^3 \zeta_3 + 2\pi^2 L^3 + 30L^2 \zeta_3 + \frac{83\pi^4 L^2}{360} - \frac{7\pi^2 L^2}{3} - 6L^2 \right. \\
& - 240L\zeta_5 - \frac{4}{3}\pi^2 L\zeta_3 + 20L\zeta_3 + \frac{19\pi^4 L}{15} + 7\pi^2 L - 50L + 16\zeta_3^2 + \frac{89\pi^2 \zeta_3}{3} \\
& - 654\zeta_3 + 424\zeta_5 + \frac{37729\pi^6}{136080} + \frac{575}{3} - \frac{353\pi^2}{18} - \frac{77\pi^4}{36} \Big] + C_F^2 C_A \left[-\frac{11L^5}{9} - \frac{\pi^2 L^4}{3} \right. \\
& + \frac{67L^4}{9} + 26L^3 \zeta_3 - \frac{308L^3}{27} - \frac{55\pi^2 L^3}{54} - \frac{943L^2 \zeta_3}{9} + \frac{689\pi^2 L^2}{108} + \frac{1673L^2}{81} - \frac{17\pi^4 L^2}{90} \\
& - \frac{5}{3}\pi^2 L\zeta_3 + \frac{1660L\zeta_3}{3} + 120L\zeta_5 + \frac{\pi^4 L}{6} + \frac{614L}{27} - \frac{3506\pi^2 L}{81} + \frac{296\zeta_3^2}{3} - \frac{1676\zeta_5}{9} \\
& - \frac{4820\zeta_3}{27} - \frac{3049\pi^2 \zeta_3}{54} + \frac{31819\pi^2}{486} - \frac{9335}{81} - \frac{893\pi^4}{9720} - \frac{3169\pi^6}{17010} \Big] + C_F^2 \left[\frac{10L^5}{9} - \frac{50L^4}{9} \right. \\
& + \frac{25\pi^2 L^3}{27} + \frac{250L^3}{27} + \frac{350L^2 \zeta_3}{9} - \frac{335\pi^2 L^2}{54} + \frac{3625L^2}{162} - \frac{4160L\zeta_3}{9} + \frac{7\pi^4 L}{9} + \frac{2200\pi^2 L}{81} \\
& - \frac{7075L}{54} + \frac{59980\zeta_3}{81} - \frac{2080\zeta_5}{9} - \frac{95\pi^2 \zeta_3}{27} - \frac{305\pi^4}{972} - \frac{30655\pi^2}{972} + \frac{179375}{972} \Big] \\
& + C_F C_A^2 \left[-\frac{121L^4}{54} - \frac{22\pi^2 L^3}{27} + \frac{1780L^3}{81} + 88L^2 \zeta_3 + \frac{13\pi^2 L^2}{27} - \frac{11\pi^4 L^2}{45} - \frac{11939L^2}{162} \right. \\
& + \frac{44}{9}\pi^2 L\zeta_3 + 136L\zeta_5 - \frac{13900L\zeta_3}{27} + \frac{4822\pi^2 L}{243} - \frac{47\pi^4 L}{54} + \frac{10289L}{1458} + \frac{163\pi^2 \zeta_3}{9} \\
& + \frac{107648\zeta_3}{243} + \frac{106\zeta_5}{9} - \frac{1136\zeta_3^2}{9} + \frac{10093\pi^4}{4860} - \frac{769\pi^6}{5103} - \frac{264515\pi^2}{8748} + \frac{5964431}{26244} \Big] \\
& + C_A C_F \left[\frac{110L^4}{27} + \frac{20\pi^2 L^3}{27} - \frac{2890L^3}{81} - 40L^2 \zeta_3 + \frac{40\pi^2 L^2}{9} + \frac{8635L^2}{81} + \frac{3620L\zeta_3}{9} \right. \\
& + \frac{11\pi^4 L}{27} - \frac{8180\pi^2 L}{243} - \frac{37495L}{729} + \frac{10\pi^2 \zeta_3}{9} - \frac{20\zeta_5}{3} - \frac{14300\zeta_3}{27} + \frac{166295\pi^2}{4374} \\
& - \frac{119\pi^4}{243} - \frac{2609875}{13122} \Big] + C_F \left[-\frac{50L^4}{27} + \frac{1000L^3}{81} - \frac{100\pi^2 L^2}{27} - \frac{2500L^2}{81} + \frac{400L\zeta_3}{27} \right. \\
& + \frac{1000\pi^2 L}{81} + \frac{23200L}{729} - \frac{5000\zeta_3}{243} - \frac{235\pi^4}{243} - \frac{2650\pi^2}{243} + \frac{51800}{6561} \Big], \tag{B4}
\end{aligned}$$

where $L = \ln [(-m_H^2 - i\epsilon)/\mu^2]$. Although not used in this paper, the fourth-order coefficients can already be extracted from the form factors calculated in Refs. [61,62].

The jet functions are expanded as

$$\tilde{j}^{q,g}(L_J, \mu) = \sum_{n=0} \left(\frac{\alpha_s}{4\pi} \right)^n \tilde{j}^{q,g(n)}(L_J). \tag{B5}$$

The expansion coefficients for the quark jet function are [12,71]

$$\begin{aligned}
\tilde{j}^{q(1)}(L_J) = & C_F \left(2L_J^2 - 3L_J - \frac{2\pi^2}{3} + 7 \right), \\
\tilde{j}^{q(2)}(L_J) = & C_F n_f \left[\frac{4}{9}L_J^3 - \frac{29}{9}L_J^2 + \left(\frac{247}{27} - \frac{2\pi^2}{9} \right)L_J + \frac{13\pi^2}{18} - \frac{4057}{324} \right] \\
& + C_F C_A \left[-\frac{22}{9}L_J^3 + \left(\frac{367}{18} - \frac{2\pi^2}{3} \right)L_J^2 + \left(40\zeta_3 + \frac{11\pi^2}{9} - \frac{3155}{54} \right)L_J - 18\zeta_3 - \frac{37\pi^4}{180} \right. \\
& \left. - \frac{155\pi^2}{36} + \frac{53129}{648} \right] + C_F^2 \left[2L_J^4 - 6L_J^3 + \left(\frac{37}{2} - \frac{4\pi^2}{3} \right)L_J^2 + \left(4\pi^2 - 24\zeta_3 - \frac{45}{2} \right)L_J - 6\zeta_3 + \frac{61\pi^4}{90} - \frac{97\pi^2}{12} + \frac{205}{8} \right],
\end{aligned}$$

$$\begin{aligned}
\tilde{j}^{q(3)}(L_J) = & C_F n_f^2 \left[\frac{4}{27} L_J^4 - \frac{116}{81} L_J^3 + \left(\frac{470}{81} - \frac{4\pi^2}{27} \right) L_J^2 + \left(\frac{58\pi^2}{81} - \frac{8714}{729} - \frac{64}{27} \zeta_3 \right) L_J \right] \\
& + C_F C_A n_f \left[-\frac{44}{27} L_J^4 + \left(\frac{1552}{81} - \frac{8\pi^2}{27} \right) L_J^3 + \left(\frac{28\pi^2}{9} - \frac{7531}{81} + 8\zeta_3 \right) L_J^2 + \left(\frac{32\pi^4}{135} \right. \right. \\
& \left. \left. - \frac{1976\zeta_3}{27} - \frac{2632\pi^2}{243} + \frac{160906}{729} \right) L_J \right] + C_F C_A^2 \left[\frac{121}{27} L_J^4 + \left(\frac{44\pi^2}{27} - \frac{4649}{81} \right) L_J^3 + \left(\frac{22\pi^4}{45} \right. \right. \\
& \left. \left. - 132\zeta_3 - \frac{389\pi^2}{27} + \frac{50689}{162} \right) L_J^2 + \left(\frac{18179\pi^2}{486} - \frac{53\pi^4}{135} - \frac{599375}{729} - 232\zeta_5 - \frac{88\pi^2\zeta_3}{9} \right. \right. \\
& \left. \left. + \frac{6688\zeta_3}{9} \right) L_J \right] + C_F^2 n_f \left[\frac{8}{9} L_J^5 - \frac{70}{9} L_J^4 + \left(\frac{875}{27} - \frac{20\pi^2}{27} \right) L_J^3 + \left(\frac{151\pi^2}{27} - \frac{15775}{162} \right) L_J^2 \right. \\
& \left. + \left(\frac{32\zeta_3}{9} + \frac{4\pi^4}{27} - \frac{2833\pi^2}{162} + \frac{7325}{36} \right) L_J \right] + C_F^2 C_A \left[-\frac{44}{9} L_J^5 + \left(\frac{433}{9} - \frac{4\pi^2}{3} \right) L_J^4 \right. \\
& \left. + \left(\frac{164\pi^2}{27} - \frac{10537}{54} + 80\zeta_3 \right) L_J^3 + \left(-68\zeta_3 + \frac{\pi^4}{30} - \frac{2045\pi^2}{54} + \frac{157943}{324} \right) L_J^2 \right. \\
& \left. + \left(\frac{290\zeta_3}{3} - 120\zeta_5 - \frac{88\pi^2\zeta_3}{3} - \frac{923\pi^4}{540} + \frac{35075\pi^2}{324} - \frac{151405}{216} \right) L_J \right] + C_F^3 \left[\frac{4}{3} L_J^6 - 6L_J^5 \right. \\
& \left. + \left(23 - \frac{4\pi^2}{3} \right) L_J^4 + \left(8\pi^2 - \frac{99}{2} - 48\zeta_3 \right) L_J^3 + \left(60\zeta_3 + \frac{61\pi^4}{45} - \frac{151\pi^2}{6} + \frac{349}{4} \right) L_J^2 \right. \\
& \left. + \left(240\zeta_5 + \frac{64\pi^2\zeta_3}{3} - 218\zeta_3 - \frac{149\pi^4}{30} + \frac{145\pi^2}{4} - \frac{815}{8} \right) L_J \right] + c_{3q}^J, \tag{B6}
\end{aligned}$$

The scale-independent constant term c_{3q}^J is given by [71]

$$\begin{aligned}
c_{3q}^J = & 25.06777873 C_F^3 + 32.81169125 C_A C_F^2 - 0.7795843561 C_A^2 C_F - 31.65196210 C_A C_F n_f T_F \\
& - 61.78995095 C_F^2 n_f T_F + 28.49157341 C_F n_f^2 T_F^2. \tag{B7}
\end{aligned}$$

The expansion coefficients for the gluon jet function are [70,72]

$$\begin{aligned}
\tilde{j}^{g(1)}(L_J) = & C_A \left(2L_J^2 - \frac{11}{3} L_J + \frac{67}{9} - \frac{2\pi^2}{3} \right) + n_f \left(\frac{2}{3} L_J - \frac{10}{9} \right), \\
\tilde{j}^{g(2)}(L_J) = & n_f^2 \left(\frac{4}{9} L_J^2 - \frac{40}{27} L_J - \frac{2\pi^2}{27} + \frac{100}{81} \right) + C_F n_f \left(2L_J + 8\zeta_3 - \frac{55}{6} \right) + C_A n_f \left[\frac{16}{9} L_J^3 \right. \\
& \left. - \frac{28}{3} L_J^2 + \left(\frac{224}{9} - \frac{10\pi^2}{9} \right) L_J - \frac{8\zeta_3}{3} + \frac{67\pi^2}{27} - \frac{760}{27} \right] + C_A^2 \left[2L_J^4 - \frac{88}{9} L_J^3 + \left(\frac{389}{9} - 2\pi^2 \right) L_J^2 \right. \\
& \left. + \left(\frac{55\pi^2}{9} + 16\zeta_3 - \frac{2570}{27} \right) L_J - \frac{88\zeta_3}{3} + \frac{17\pi^4}{36} - \frac{362\pi^2}{27} + \frac{20215}{162} \right], \\
\tilde{j}^{g(3)}(L_J) = & n_f^3 \left[\frac{8}{27} L_J^3 - \frac{40}{27} L_J^2 + \left(\frac{200}{81} - \frac{4\pi^2}{27} \right) L_J \right] + C_F n_f^2 \left[\frac{10}{3} L_J^2 + (16\zeta_3 - 24) L_J \right] \\
& - C_F^2 n_f L_J + C_A n_f^2 \left[\frac{4}{3} L_J^4 - \frac{292}{27} L_J^3 + \left(\frac{3326}{81} - \frac{4\pi^2}{3} \right) L_J^2 + \left(\frac{508\pi^2}{81} - \frac{116509}{1458} - \frac{256\zeta_3}{27} \right) L_J \right] \\
& + C_A C_F n_f \left[\frac{16}{3} L_J^3 + (32\zeta_3 - 55) L_J^2 + \left(-\frac{8\pi^4}{45} - \frac{10\pi^2}{3} + \frac{5599}{27} - \frac{1096\zeta_3}{9} \right) L_J \right]
\end{aligned}$$

$$\begin{aligned}
& + C_A^2 n_f \left[\frac{20}{9} L_J^5 - \frac{64}{3} L_J^4 - \left(\frac{88\pi^2}{27} - \frac{3106}{27} \right) L_J^3 + \left(\frac{586\pi^2}{27} - \frac{8\zeta_3}{3} - \frac{10067}{27} \right) L_J^2 \right. \\
& + \left. \left(\frac{449\pi^4}{270} - \frac{16831\pi^2}{243} + \frac{1052135}{1458} - \frac{1280\zeta_3}{27} \right) L_J \right] + C_A^3 \left[\frac{4}{3} L_J^6 - \frac{110}{9} L_J^5 + \left(85 - \frac{8\pi^2}{3} \right) L_J^4 \right. \\
& + \left. \left(\frac{484\pi^2}{27} - \frac{9623}{27} + 32\zeta_3 \right) L_J^3 + \left(\frac{169\pi^4}{90} - \frac{484\zeta_3}{3} - \frac{2362\pi^2}{27} + \frac{85924}{81} \right) L_J^2 \right. \\
& + \left. \left(-\frac{4411\pi^4}{540} + \frac{52678\pi^2}{243} - \frac{1448021}{729} - 112\zeta_5 - \frac{160\pi^2\zeta_3}{9} + \frac{6316\zeta_3}{9} \right) L_J \right] + c_{3g}^J. \tag{B8}
\end{aligned}$$

From Ref. [72], we have $c_{3g}^J = 647.7843434644$ for $n_f = 5$.

The soft functions are expanded as

$$\tilde{s}_{q,g}(L_S, \mu) = \sum_{n=0} \left(\frac{\alpha_s}{4\pi} \right)^n \tilde{s}^{q,g(n)}(L_S). \tag{B9}$$

The expansion coefficients for the quark soft function are [12,80]

$$\begin{aligned}
\tilde{s}^{q(1)}(L_S) &= C_F(-8L_S^2 - \pi^2), \\
\tilde{s}^{q(2)}(L_S) &= C_F n_f \left[-\frac{32}{9} L_S^3 + \frac{80}{9} L_S^2 - \left(\frac{8\pi^2}{9} + \frac{224}{27} \right) L_S - \frac{52\zeta_3}{9} + \frac{77\pi^2}{27} + \frac{40}{81} \right] \\
&+ C_F C_A \left[\frac{176}{9} L_S^3 + \left(\frac{8\pi^2}{3} - \frac{536}{9} \right) L_S^2 + \left(\frac{44\pi^2}{9} - 56\zeta_3 + \frac{1616}{27} \right) L_S + \frac{286\zeta_3}{9} + \frac{14\pi^4}{15} \right. \\
&\left. - \frac{871\pi^2}{54} - \frac{2140}{81} \right] + C_F^2 \left(32L_S^4 + 8\pi^2 L_S^2 + \frac{\pi^4}{2} \right), \\
\tilde{s}^{q(3)}(L_S) &= C_F n_f^2 \left[-\frac{64}{27} L_S^4 + \frac{640}{81} L_S^3 - \left(\frac{32\pi^2}{27} + \frac{800}{81} \right) L_S^2 + \left(\frac{64\pi^2}{9} - \frac{3200}{729} - \frac{64\zeta_3}{9} \right) L_S \right] \\
&+ C_F C_A n_f \left[\frac{704}{27} L_S^4 + \left(\frac{64\pi^2}{27} - \frac{9248}{81} \right) L_S^3 + \left(\frac{64\pi^2}{9} + \frac{16408}{81} \right) L_S^2 + \left(\frac{6032\zeta_3}{27} + \frac{64\pi^4}{45} \right. \right. \\
&\left. \left. - \frac{19408\pi^2}{243} - \frac{80324}{729} \right) L_S \right] + C_F C_A^2 \left[-\frac{1936}{27} L_S^4 - \left(\frac{352\pi^2}{27} - \frac{28480}{81} \right) L_S^3 + \left(\frac{104\pi^2}{27} \right. \right. \\
&\left. \left. - \frac{88\pi^4}{45} - \frac{62012}{81} + 352\zeta_3 \right) L_S^2 + \left(\frac{50344\pi^2}{243} - \frac{88\pi^4}{9} + \frac{556042}{729} + 384\zeta_5 + \frac{176\pi^2\zeta_3}{9} \right. \right. \\
&\left. \left. - \frac{36272\zeta_3}{27} \right) L_S \right] + C_F^2 n_f \left[\frac{256}{9} L_S^5 - \frac{640}{9} L_S^4 + \left(\frac{32\pi^2}{3} + \frac{1504}{27} \right) L_S^3 + \left(\frac{5620}{81} - \frac{856\pi^2}{27} \right. \right. \\
&\left. \left. - \frac{160\zeta_3}{9} \right) L_S^2 + \left(\frac{608\zeta_3}{9} + \frac{56\pi^4}{45} + \frac{152\pi^2}{27} - \frac{3422}{27} \right) L_S \right] + C_F^2 C_A \left[-\frac{1408}{9} L_S^5 \right. \\
&+ \left(\frac{4288}{9} - \frac{64\pi^2}{3} \right) L_S^4 + \left(448\zeta_3 - \frac{176\pi^2}{3} - \frac{12928}{27} \right) L_S^3 + \left(\frac{5092\pi^2}{27} - \frac{2288\zeta_3}{9} - \frac{152\pi^4}{15} \right. \\
&\left. + \frac{17120}{81} \right) L_S^2 + \left(56\pi^2\zeta_3 - \frac{44\pi^4}{9} - \frac{1616\pi^2}{27} \right) L_S \left. \right] + C_F^3 \left[-\frac{256}{3} L_S^6 - 32\pi^2 L_S^4 - 4\pi^4 L_S^2 \right] + c_{3g}^S. \tag{B10}
\end{aligned}$$

The three-loop scale-independent term c_{3g}^S is not precisely known at the moment. Its calculation is under active investigation [84,91,92]. In Ref. [71], this term was extracted through a numeric fit to the fixed-order thrust distribution. The value (with large uncertainties) reads

$$c_{3q}^S = -19988 \pm 1440(\text{stat}) \pm 4000(\text{syst}). \quad (\text{B11})$$

The results for the gluon soft function can be obtained from the quark one employing the non-Abelian exponential theorem [93–95]. Up to three loops, they are related by the Casimir scaling

$$\ln [\tilde{s}^g(L_S, \mu)] = \frac{C_A}{C_F} \ln [\tilde{s}^q(L_S, \mu)]. \quad (\text{B12})$$

Hence the expansion coefficients for the gluon soft function are

$$\begin{aligned} \tilde{s}^{g(1)}(L_S) &= C_A(-8L_S^2 - \pi^2), \\ \tilde{s}^{g(2)}(L_S) &= C_A n_f \left[-\frac{32}{9} L_S^3 + \frac{80}{9} L_S^2 - \left(\frac{8\pi^2}{9} + \frac{224}{27} \right) L_S + \frac{77\pi^2}{27} + \frac{40}{81} - \frac{52\zeta_3}{9} \right] \\ &\quad + C_A^2 \left[32L_S^4 + \frac{176}{9} L_S^3 + \left(\frac{32\pi^2}{3} - \frac{536}{9} \right) L_S^2 + \left(\frac{44\pi^2}{9} + \frac{1616}{27} - 56\zeta_3 \right) L_S + \frac{286\zeta_3}{9} \right. \\ &\quad \left. + \frac{43\pi^4}{30} - \frac{871\pi^2}{54} - \frac{2140}{81} \right], \\ \tilde{s}^{g(3)}(L_S) &= C_A n_f^2 \left[-\frac{64}{27} L_S^4 + \frac{640}{81} L_S^3 - \left(\frac{32\pi^2}{27} + \frac{800}{81} \right) L_S^2 + \left(\frac{64\pi^2}{9} - \frac{3200}{729} - \frac{64\zeta_3}{9} \right) L_S \right] \\ &\quad + C_F C_A n_f \left[-\frac{32}{3} L_S^3 + \left(\frac{220}{3} - 64\zeta_3 \right) L_S^2 + \left(\frac{608\zeta_3}{9} + \frac{16\pi^4}{45} - \frac{8\pi^2}{3} - \frac{3422}{27} \right) L_S \right] \\ &\quad + C_A^2 n_f \left[\frac{256}{9} L_S^5 - \frac{1216}{27} L_S^4 + \left(\frac{352\pi^2}{27} - \frac{3872}{81} \right) L_S^3 + \left(\frac{416\zeta_3}{9} - \frac{664\pi^2}{27} + \frac{16088}{81} \right) L_S^2 \right. \\ &\quad \left. + \left(\frac{6032\zeta_3}{27} + \frac{104\pi^4}{45} - \frac{17392\pi^2}{243} - \frac{80324}{729} \right) L_S \right] + C_A^3 \left[-\frac{256}{3} L_S^6 - \frac{1408}{9} L_S^5 \right. \\ &\quad \left. + \left(\frac{10928}{27} - \frac{160\pi^2}{3} \right) L_S^4 + \left(448\zeta_3 - \frac{1936\pi^2}{27} - \frac{10304}{81} \right) L_S^3 + \left(\frac{880\zeta_3}{9} - \frac{724\pi^4}{45} \right. \right. \\ &\quad \left. \left. + \frac{1732\pi^2}{9} - \frac{4988}{9} \right) L_S^2 + \left(\frac{680\pi^2\zeta_3}{9} - \frac{36272\zeta_3}{27} + 384\zeta_5 - \frac{44\pi^4}{3} + \frac{35800\pi^2}{243} + \frac{556042}{729} \right) L_S \right] + c_{3g}^S, \quad (\text{B13}) \end{aligned}$$

where

$$\begin{aligned} c_{3g}^S &= C_A C_F n_f \left(-\frac{52}{9} \pi^2 \zeta_3 + \frac{77\pi^4}{27} + \frac{40\pi^2}{81} \right) + C_A^2 n_f \left(\frac{52\pi^2\zeta_3}{9} - \frac{77\pi^4}{27} - \frac{40\pi^2}{81} \right) \\ &\quad + C_A^3 \left(-\frac{286}{9} \pi^2 \zeta_3 - \frac{11\pi^6}{10} + \frac{871\pi^4}{54} + \frac{2140\pi^2}{81} \right) + C_A^2 C_F \left(\frac{286\pi^2\zeta_3}{9} + \frac{14\pi^6}{15} \right. \\ &\quad \left. - \frac{871\pi^4}{54} - \frac{2140\pi^2}{81} \right) + C_A C_F^2 \frac{1}{6} \pi^6 + \frac{C_A}{C_F} c_{3q}^S. \quad (\text{B14}) \end{aligned}$$

APPENDIX C: ANOMALOUS DIMENSIONS

In this appendix we list the expressions of the various anomalous dimensions appearing in the resummation formula.

For the cusp anomalous dimensions, we write

$$\begin{aligned} \Gamma_{\text{cusp}}^q(\alpha_s) &= C_F [\gamma_{\text{cusp}}(\alpha_s) + \delta\gamma_{\text{cusp}}^q(\alpha_s)], \\ \Gamma_{\text{cusp}}^g(\alpha_s) &= C_A [\gamma_{\text{cusp}}(\alpha_s) + \delta\gamma_{\text{cusp}}^g(\alpha_s)]. \quad (\text{C1}) \end{aligned}$$

Up to three loops the cusp anomalous dimensions satisfy Casimir scaling, so that $\delta\gamma_{\text{cusp}}^q(\alpha_s)$ and $\delta\gamma_{\text{cusp}}^g(\alpha_s)$ only start at α_s^4 . We define the expansion as

$$\begin{aligned} \gamma_{\text{cusp}}(\alpha_s) &= \sum_{n=0} \gamma_{\text{cusp}}^{(n)} \left(\frac{\alpha_s}{4\pi} \right)^{n+1}, \\ \delta\gamma_{\text{cusp}}^{q,g}(\alpha_s) &= \sum_{n=3} \delta\gamma_{\text{cusp}}^{q,g(n)} \left(\frac{\alpha_s}{4\pi} \right)^{n+1}. \quad (\text{C2}) \end{aligned}$$

The expansion coefficients are [31,33–35]

$$\begin{aligned}
\gamma_{\text{cusp}}^{(0)} &= 4, \\
\gamma_{\text{cusp}}^{(1)} &= -\frac{1}{3}4\pi^2 C_A + \frac{268C_A}{9} - \frac{80n_f T_F}{9}, \\
\gamma_{\text{cusp}}^{(2)} &= -\frac{16n_f^2}{27} - \frac{208n_f\zeta(3)}{3} + \frac{80\pi^2 n_f}{9} - \frac{1276n_f}{9} + 264\zeta_3 + \frac{44\pi^4}{5} - \frac{536\pi^2}{3} + 1470n_f, \\
\gamma_{\text{cusp}}^{(3)} &= n_f^3 \left(\frac{64\zeta_3}{27} - \frac{32}{81} \right) + n_f^2 \left(\frac{4160\zeta_3}{27} - \frac{304\pi^2}{81} - \frac{104\pi^4}{135} + \frac{17875}{243} \right) + n_f \left(\frac{416\pi^2\zeta_3}{3} \right. \\
&\quad \left. - \frac{153920\zeta_3}{27} + \frac{19504\zeta_5}{9} + \frac{12800\pi^2}{27} - \frac{616\pi^4}{45} - \frac{344345}{81} \right) - 432\zeta_3^2 - 528\pi^2\zeta_3 \\
&\quad + 20944\zeta_3 - 10824\zeta_5 + \frac{2706\pi^4}{5} + \frac{84278}{3} - \frac{44200\pi^2}{9} - \frac{2504\pi^6}{105}, \\
\delta\gamma_{\text{cusp}}^{q(3)} &= n_f \left(-\frac{80\zeta_3}{9} - \frac{400\zeta_5}{9} + \frac{40\pi^2}{9} \right) - 720\zeta_3^2 + 80\zeta_3 + 2200\zeta_5 - 40\pi^2 - \frac{124\pi^6}{63}, \\
\delta\gamma_{\text{cusp}}^{g(3)} &= n_f \left(-\frac{80\zeta_3}{3} - \frac{400\zeta_5}{3} + \frac{40\pi^2}{3} \right) - 2160\zeta_3^2 + 240\zeta_3 + 6600\zeta_5 - 120\pi^2 - \frac{124\pi^6}{21}. \tag{C3}
\end{aligned}$$

As far as we know, there are no complete results for the five-loop cusp anomalous dimensions. In this paper, we make use of the approximate results estimated in [35],

$$\begin{aligned}
\gamma_{\text{cusp}}^{(4)} + \delta\gamma_{\text{cusp}}^{q(4)} &= 50000 \pm 40000, \\
\gamma_{\text{cusp}}^{(4)} + \delta\gamma_{\text{cusp}}^{g(4)} &= 30000 \pm 60000. \tag{C4}
\end{aligned}$$

The anomalous dimension for the quark Yukawa coupling reads

$$\gamma_y = -\sum_{n=0} \left(\frac{\alpha_s}{4\pi} \right)^{n+1} \gamma_y^{(n)}, \tag{C5}$$

where [44,45]

$$\begin{aligned}
\gamma_y^{(0)} &= 6C_F, \\
\gamma_y^{(1)} &= \frac{97C_A C_F}{3} - \frac{10C_F n_f}{3} + 3C_F^2, \\
\gamma_y^{(2)} &= -48\zeta_3 C_A C_F n_f - \frac{556}{27} C_A C_F n_f - \frac{129}{2} C_A C_F^2 + \frac{11413}{54} C_A^2 C_F + 48\zeta_3 C_F^2 n_f - 46C_F^2 n_f - \frac{70}{27} C_F n_f^2 + 129C_F^3, \\
\gamma_y^{(3)} &= n_f^3 \left(\frac{128\zeta_3}{27} - \frac{664}{243} \right) + n_f^2 \left(\frac{1600\zeta_3}{9} - \frac{32\pi^4}{27} + \frac{10484}{243} \right) + n_f \left(-\frac{68384\zeta_3}{9} + \frac{36800\zeta_5}{9} + \frac{176\pi^4}{9} - \frac{183446}{27} \right) \\
&\quad + \frac{271360\zeta_3}{27} - 17600\zeta_5 + \frac{4603055}{81}. \tag{C6}
\end{aligned}$$

The anomalous dimension for the Wilson coefficient C_t is

$$\gamma_t(\alpha_s) = \sum_{n=0} \left(\frac{\alpha_s}{4\pi} \right)^{n+1} \gamma_t^{(n)}, \tag{C7}$$

where [47–51]

$$\begin{aligned}\gamma_t^{(0)} &= 0, \\ \gamma_t^{(1)} &= \frac{40}{3} C_A n_f T_F - \frac{1}{3} 68 C_A^2 + 8 C_F n_f T_F, \\ \gamma_t^{(2)} &= -\frac{1}{27} 650 n_f^2 + \frac{10066 n_f}{9} - 5714, \\ \gamma_t^{(2)} &= -\frac{2186 n_f^3}{243} + n_f^2 \left(-\frac{12944 \zeta_3}{27} - \frac{50065}{27} \right) + n_f \left(\frac{13016 \zeta_3}{9} + \frac{1078361}{27} \right) - 21384 \zeta_3 - 149753.\end{aligned}\quad (\text{C8})$$

The anomalous dimension for the jet functions are

$$\gamma_j^{q,g}(\alpha_s) = \sum_{n=0} \left(\frac{\alpha_s}{4\pi} \right)^{n+1} \gamma_j^{q,g(n)}, \quad (\text{C9})$$

where [66,81]

$$\begin{aligned}\gamma_j^{q(0)} &= -3 C_F, \\ \gamma_j^{q(1)} &= \frac{8\pi^2 n_f}{27} + \frac{484 n_f}{81} + \frac{352 \zeta_3}{3} - \frac{4\pi^2}{3} - \frac{3610}{27}, \\ \gamma_j^{q(2)} &= -\frac{256}{81} \zeta_3 n_f^2 - \frac{14272 \zeta_3 n_f}{81} - \frac{80}{243} \pi^2 n_f^2 + \frac{13828 n_f^2}{2187} + \frac{1172 \pi^4 n_f}{1215} + \frac{1592 \pi^2 n_f}{243} \\ &\quad + \frac{100984 n_f}{729} - \frac{25696 \zeta_5}{9} - \frac{9632 \pi^2 \zeta_3}{81} + \frac{153136 \zeta(3)}{27} - \frac{6818 \pi^4}{405} + \frac{7588 \pi^2}{81} - \frac{470183}{243}, \\ \gamma_j^{q(3)} &= 4483.56,\end{aligned}\quad (\text{C10})$$

and [66,70]

$$\begin{aligned}\gamma_j^{g(0)} &= -\beta_0, \\ \gamma_j^{g(1)} &= -\frac{2}{9} \pi^2 n_f C_A + \frac{184 n_f C_A}{27} + 16 \zeta_3 C_A^2 + \frac{11}{9} \pi^2 C_A^2 - \frac{1096 C_A^2}{27} + 2 n_f C_F, \\ \gamma_j^{g(2)} &= -\frac{304}{9} n_f \zeta_3 C_A C_F - \frac{8}{45} \pi^4 n_f C_A C_F - \frac{2}{3} \pi^2 n_f C_A C_F + \frac{4145}{54} n_f C_A C_F - \frac{112}{27} n_f^2 \zeta_3 C_A \\ &\quad + \frac{1811 n_f^2 C_A}{1458} + \frac{20}{81} \pi^2 n_f^2 C_A - \frac{8}{27} n_f \zeta_3 C_A^2 + \frac{77}{135} \pi^4 n_f C_A^2 - \frac{1306}{243} \pi^2 n_f C_A^2 \\ &\quad + \frac{42557 n_f C_A^2}{1458} - \frac{64}{9} \pi^2 \zeta_3 C_A^3 + 260 \zeta_3 C_A^3 - 112 \zeta_5 C_A^3 + \frac{6217}{243} \pi^2 C_A^3 - \frac{583}{270} \pi^4 C_A^3 \\ &\quad - \frac{331153 C_A^3}{1458} - \frac{11 n_f^2 C_F}{9} - n_f C_F^2, \\ \gamma_j^{g(3)} &= 26138.7.\end{aligned}\quad (\text{C11})$$

The hard anomalous dimensions are

$$\gamma_H^{q,g}(\alpha_s) = \sum_{n=0} \left(\frac{\alpha_s}{4\pi} \right)^{n+1} \gamma_H^{q,g(n)}, \quad (\text{C12})$$

where the coefficients up to three loops can be obtained from Eqs. (B3) and (B4). For the gluon case, they read [53–57,59,62]

$$\begin{aligned}
\gamma_H^{g(0)} &= 0, \\
\gamma_H^{g(1)} &= -\frac{2\pi^2 n_f}{3} - \frac{152 n_f}{9} + 36\zeta_3 + 11\pi^2 - \frac{160}{3}, \\
\gamma_H^{g(2)} &= -\frac{112 n_f^2 \zeta_3}{9} + \frac{20\pi^2 n_f^2}{27} + \frac{7714 n_f^2}{243} + \frac{920 n_f \zeta_3}{9} + \frac{214\pi^4 n_f}{45} - \frac{1270\pi^2 n_f}{27} \\
&\quad - \frac{76256 n_f}{81} - 120\pi^2 \zeta_3 + 2196\zeta_3 - 864\zeta_5 + \frac{6109\pi^2}{9} - \frac{319\pi^4}{5} + \frac{37045}{27}, \\
\gamma_H^{g(3)} &= n_f^3 \left(\frac{400\zeta_3}{81} + \frac{8\pi^2}{81} - \frac{64\pi^4}{405} + \frac{38426}{2187} \right) + n_f^2 \left(\frac{368\pi^2 \zeta_3}{9} - \frac{49342\zeta_3}{81} \right. \\
&\quad \left. + \frac{8000\zeta_5}{9} + \frac{19675\pi^2}{486} - \frac{2474\pi^4}{405} + \frac{3605645}{1944} \right) + n_f \left(\frac{32\zeta_3^2}{3} - 504\pi^2 \zeta_3 \right. \\
&\quad \left. + \frac{528362\zeta_3}{27} - \frac{90140\zeta_5}{9} + \frac{52153\pi^4}{135} - \frac{262193\pi^2}{162} - \frac{7927313}{216} - \frac{54917\pi^6}{2835} \right) \\
&\quad + 21384\zeta_3^2 + \frac{2004\pi^4 \zeta_3}{5} - 576\pi^2 \zeta_3 + \frac{119536\zeta_3}{3} + 1152\pi^2 \zeta_5 \\
&\quad - 62796\zeta_5 - 22734\zeta_7 + \frac{18051\pi^6}{70} + \frac{1041691\pi^2}{54} - \frac{123029\pi^4}{30} + \frac{5481844}{81}. \tag{C13}
\end{aligned}$$

For the quark case, they are given as [53,60,61,96]

$$\begin{aligned}
\gamma_H^{q(0)} &= 0, \\
\gamma_H^{q(1)} &= \frac{8\pi^2 n_f}{9} + \frac{160 n_f}{81} + \frac{368\zeta_3}{3} - \frac{68\pi^2}{9} - \frac{352}{27}, \\
\gamma_H^{q(2)} &= -\frac{64 n_f^2 \zeta_3}{81} - \frac{80\pi^2 n_f^2}{81} + \frac{11776 n_f^2}{2187} - \frac{23584 n_f \zeta_3}{81} + \frac{136\pi^4 n_f}{1215} + \frac{9128\pi^2 n_f}{243} \\
&\quad - \frac{47192 n_f}{729} + \frac{164144\zeta_3}{27} - \frac{30656\zeta_5}{9} - \frac{9760\pi^2 \zeta_3}{81} - \frac{10124\pi^2}{81} + \frac{213772}{243} - \frac{4132\pi^4}{405}, \\
\gamma_s^{q(3)} &= n_f^3 \left(-\frac{2240\zeta_3}{729} - \frac{32\pi^2}{243} - \frac{128\pi^4}{3645} + \frac{95744}{19683} \right) + n_f^2 \left(-\frac{1}{243} 2816\pi^2 \zeta_3 \right. \\
&\quad \left. + \frac{18848\zeta_3}{729} + \frac{25984\zeta_5}{81} + \frac{6856\pi^4}{10935} - \frac{130486\pi^2}{2187} + \frac{126461}{4374} \right) + n_f \left(-\frac{110848\zeta_3^2}{27} \right. \\
&\quad \left. + \frac{115504\pi^2 \zeta_3}{243} - \frac{3066064\zeta_3}{243} + \frac{59488\zeta_5}{9} + \frac{29264\pi^4}{729} + \frac{755786\pi^2}{729} - \frac{1641457}{486} \right. \\
&\quad \left. - \frac{975668\pi^6}{229635} \right) + \frac{175712\zeta_3^2}{9} + \frac{992696\pi^4 \zeta_3}{3645} + \frac{1365152\zeta_3}{9} + \frac{243872\pi^2 \zeta_5}{81} \\
&\quad + \frac{2888332\zeta_7}{27} - \frac{81584\pi^2 \zeta_3}{9} - \frac{2158832\zeta_5}{9} + \frac{2058794\pi^6}{25515} - \frac{362842\pi^2}{243} + \frac{19161124}{729} - \frac{1095218\pi^4}{1215}. \tag{C14}
\end{aligned}$$

Due to the RG invariance of physical observables, the soft anomalous dimensions satisfy the consistency relations

$$\begin{aligned}
\gamma_s^q &= \gamma_H^q + \gamma_y - 2\gamma_j^q, \\
\gamma_s^g &= \gamma_H^g + \gamma_t + \frac{\beta}{\alpha_s} - 2\gamma_j^g. \tag{C15}
\end{aligned}$$

We expand them in α_s as

$$\gamma_s^{q,g}(\alpha_s) = \sum_{n=0} \left(\frac{\alpha_s}{4\pi} \right)^{n+1} \gamma_s^{q,g(n)}, \quad (C16)$$

where

$$\begin{aligned} \gamma_s^{q(0)} &= 0, \\ \gamma_s^{q(1)} &= \frac{8\pi^2 n_f}{27} - \frac{448n_f}{81} - 112\zeta_3 - \frac{44\pi^2}{9} + \frac{3232}{27}, \\ \gamma_s^{q(2)} &= \frac{448\zeta_3 n_f^2}{81} + \frac{13600\zeta_3 n_f}{81} - \frac{80}{243}\pi^2 n_f^2 - \frac{8320n_f^2}{2187} - \frac{736\pi^4 n_f}{405} + \frac{5944\pi^2 n_f}{243} \\ &\quad - \frac{129496n_f}{729} + 2304\zeta_5 + \frac{352\pi^2 \zeta_3}{3} - 5264\zeta_3 + \frac{352\pi^4}{15} - \frac{25300\pi^2}{81} + \frac{547124}{243}, \\ \gamma_s^{q(3)} &= -5350.4, \end{aligned} \quad (C17)$$

and

$$\begin{aligned} \gamma_s^{g(0)} &= 0, \\ \gamma_s^{g(1)} &= \frac{2\pi^2 n_f}{3} - \frac{112n_f}{9} - 252\zeta_3 - 11\pi^2 + \frac{808}{3}, \\ \gamma_s^{g(2)} &= \frac{112n_f^2 \zeta_3}{9} - \frac{20\pi^2 n_f^2}{27} - \frac{2080n_f^2}{243} + \frac{3400n_f \zeta_3}{9} + \frac{1486\pi^2 n_f}{27} - \frac{184\pi^4 n_f}{45} \\ &\quad - \frac{32374n_f}{81} + 264\pi^2 \zeta_3 - 11844\zeta_3 + 5184\zeta_5 + \frac{264\pi^4}{5} - \frac{6325\pi^2}{9} + \frac{136781}{27}, \\ \gamma_s^{g(3)} &= -14715.4. \end{aligned} \quad (C18)$$

Up to three loops, the quark and gluon soft anomalous dimensions satisfy the Casimir scaling $\gamma_s^g/C_A = \gamma_s^q/C_F$. However, starting at four loops, due to the emergence of new Casimir operators, the relation must be generalized as appropriate [66,97].

Finally, the beta function coefficients are [40,41]

$$\begin{aligned} \beta_0 &= \frac{11C_A}{3} - \frac{4n_f T_F}{3}, \\ \beta_1 &= \frac{34C_A^2}{3} - \frac{20C_A n_f T_F}{3} - 4C_F n_f T_F, \\ \beta_2 &= \frac{325n_f^2}{54} - \frac{5033n_f}{18} + \frac{2857}{2}, \\ \beta_3 &= \frac{1093n_f^3}{729} + n_f^2 \left(\frac{6472\zeta_3}{81} + \frac{50065}{162} \right) + n_f \left(-\frac{6508\zeta_3}{27} - \frac{1078361}{162} \right) + 3564\zeta_3 + \frac{149753}{6}, \\ \beta_4 &= n_f^4 \left(\frac{1205}{2916} - \frac{152\zeta_3}{81} \right) + n_f^3 \left(-\frac{48722\zeta_3}{243} + \frac{460\zeta_5}{9} + \frac{809\pi^4}{1215} - \frac{630559}{5832} \right) \\ &\quad + n_f^2 \left(\frac{698531\zeta_3}{81} - \frac{381760\zeta_5}{81} - \frac{5263\pi^4}{405} + \frac{25960913}{1944} \right) + n_f \left(-\frac{4811164\zeta_3}{81} \right. \\ &\quad \left. + \frac{1358995\zeta_5}{27} + \frac{6787\pi^4}{108} - \frac{336460813}{1944} \right) + \frac{621885\zeta_3}{2} - 288090\zeta_5 + \frac{8157455}{16} - \frac{9801\pi^4}{20}. \end{aligned} \quad (C19)$$

- [1] G. F. Giudice and O. Lebedev, *Phys. Lett. B* **665**, 79 (2008).
- [2] F. Bishara, J. Brod, P. Uttayarat, and J. Zupan, *J. High Energy Phys.* 01 (2016) 010.
- [3] H. Baer *et al.*, arXiv:1306.6352.
- [4] A. Arbey *et al.*, *Eur. Phys. J. C* **75**, 371 (2015).
- [5] M. Dong *et al.* (CEPC Study Group), arXiv:1811.10545.
- [6] P. Bambade *et al.*, arXiv:1903.01629.
- [7] A. Abada *et al.* (FCC Collaboration), *Eur. Phys. J. Spec. Top.* **228**, 261 (2019).
- [8] E. Farhi, *Phys. Rev. Lett.* **39**, 1587 (1977).
- [9] J. Gao, Y. Gong, W.-L. Ju, and L. L. Yang, *J. High Energy Phys.* 03 (2019) 030.
- [10] S. Catani, L. Trentadue, G. Turnock, and B. R. Webber, *Nucl. Phys.* **B407**, 3 (1993).
- [11] M. D. Schwartz, *Phys. Rev. D* **77**, 014026 (2008).
- [12] T. Becher and M. D. Schwartz, *J. High Energy Phys.* 07 (2008) 034.
- [13] G. Dissertori, A. Gehrmann-De Ridder, T. Gehrmann, E. W. N. Glover, G. Heinrich, G. Luisoni, and H. Stenzel, *J. High Energy Phys.* 08 (2009) 036.
- [14] R. Abbate, M. Fickinger, A. H. Hoang, V. Mateu, and I. W. Stewart, *Phys. Rev. D* **83**, 074021 (2011).
- [15] P. F. Monni, T. Gehrmann, and G. Luisoni, *J. High Energy Phys.* 08 (2011) 010.
- [16] A. Banfi, H. McAslan, P. F. Monni, and G. Zanderighi, *J. High Energy Phys.* 05 (2015) 102.
- [17] A. H. Hoang, D. W. Kolodrubetz, V. Mateu, and I. W. Stewart, *Phys. Rev. D* **91**, 094017 (2015).
- [18] G. Bell, A. Hornig, C. Lee, and J. Talbert, *J. High Energy Phys.* 01 (2019) 147.
- [19] J. Mo, F. J. Tackmann, and W. J. Waalewijn, *Eur. Phys. J. C* **77**, 770 (2017).
- [20] S. Alioli, A. Broggio, A. Gavardi, S. Kallweit, M. A. Lim, R. Nagar, D. Napoletano, and L. Rottoli, *J. High Energy Phys.* 04 (2021) 254.
- [21] S. Catani, G. Turnock, B. R. Webber, and L. Trentadue, *Phys. Lett. B* **263**, 491 (1991).
- [22] H. Contopanagos, E. Laenen, and G. F. Sterman, *Nucl. Phys.* **B484**, 303 (1997).
- [23] N. Kidonakis, G. Oderda, and G. F. Sterman, *Nucl. Phys.* **B525**, 299 (1998).
- [24] C. F. Berger, T. Kucs, and G. F. Sterman, *Phys. Rev. D* **68**, 014012 (2003).
- [25] C. W. Bauer, S. Fleming, and M. E. Luke, *Phys. Rev. D* **63**, 014006 (2000).
- [26] C. W. Bauer, S. Fleming, D. Pirjol, and I. W. Stewart, *Phys. Rev. D* **63**, 114020 (2001).
- [27] C. W. Bauer and I. W. Stewart, *Phys. Lett. B* **516**, 134 (2001).
- [28] C. W. Bauer, S. Fleming, D. Pirjol, I. Z. Rothstein, and I. W. Stewart, *Phys. Rev. D* **66**, 014017 (2002).
- [29] C. W. Bauer, D. Pirjol, and I. W. Stewart, *Phys. Rev. D* **65**, 054022 (2002).
- [30] M. Beneke, A. P. Chapovsky, M. Diehl, and T. Feldmann, *Nucl. Phys.* **B643**, 431 (2002).
- [31] S. Moch, J. A. M. Vermaseren, and A. Vogt, *Nucl. Phys.* **B688**, 101 (2004).
- [32] A. Vogt, S. Moch, and J. A. M. Vermaseren, *Nucl. Phys.* **B691**, 129 (2004).
- [33] J. M. Henn, G. P. Korchemsky, and B. Mistlberger, *J. High Energy Phys.* 04 (2020) 018.
- [34] A. von Manteuffel, E. Panzer, and R. M. Schabinger, *Phys. Rev. Lett.* **124**, 162001 (2020).
- [35] F. Herzog, S. Moch, B. Ruijl, T. Ueda, J. A. M. Vermaseren, and A. Vogt, *Phys. Lett. B* **790**, 436 (2019).
- [36] W. E. Caswell, *Phys. Rev. Lett.* **33**, 244 (1974).
- [37] D. R. T. Jones, *Nucl. Phys.* **B75**, 531 (1974).
- [38] O. V. Tarasov, A. A. Vladimirov, and A. Y. Zharkov, *Phys. Lett.* **93B**, 429 (1980).
- [39] S. A. Larin and J. A. M. Vermaseren, *Phys. Lett. B* **303**, 334 (1993).
- [40] T. van Ritbergen, J. A. M. Vermaseren, and S. A. Larin, *Phys. Lett. B* **400**, 379 (1997).
- [41] M. Czakon, *Nucl. Phys.* **B710**, 485 (2005).
- [42] R. Tarrach, *Nucl. Phys.* **B183**, 384 (1981).
- [43] S. A. Larin, *Phys. Lett. B* **303**, 113 (1993).
- [44] J. A. M. Vermaseren, S. A. Larin, and T. van Ritbergen, *Phys. Lett. B* **405**, 327 (1997).
- [45] K. G. Chetyrkin, *Phys. Lett. B* **404**, 161 (1997).
- [46] P. A. Baikov, K. G. Chetyrkin, and J. H. Kühn, *J. High Energy Phys.* 10 (2014) 076.
- [47] V. P. Spiridonov, Report No. IYaI-P-0378, 1984.
- [48] M. Kramer, E. Laenen, and M. Spira, *Nucl. Phys.* **B511**, 523 (1998).
- [49] K. G. Chetyrkin, B. A. Kniehl, and M. Steinhauser, *Nucl. Phys.* **B510**, 61 (1998).
- [50] Y. Schroder and M. Steinhauser, *J. High Energy Phys.* 01 (2006) 051.
- [51] K. G. Chetyrkin, J. H. Kuhn, and C. Sturm, *Nucl. Phys.* **B744**, 121 (2006).
- [52] T. Liu and M. Steinhauser, *Phys. Lett. B* **746**, 330 (2015).
- [53] S. Dawson, *Nucl. Phys.* **B359**, 283 (1991).
- [54] A. Djouadi, M. Spira, and P. M. Zerwas, *Phys. Lett. B* **264**, 440 (1991).
- [55] R. V. Harlander, *Phys. Lett. B* **492**, 74 (2000).
- [56] S. Moch, J. A. M. Vermaseren, and A. Vogt, *Phys. Lett. B* **625**, 245 (2005).
- [57] T. Gehrmann, T. Huber, and D. Maitre, *Phys. Lett. B* **622**, 295 (2005).
- [58] P. A. Baikov, K. G. Chetyrkin, A. V. Smirnov, V. A. Smirnov, and M. Steinhauser, *Phys. Rev. Lett.* **102**, 212002 (2009).
- [59] T. Gehrmann, E. W. N. Glover, T. Huber, N. Ikizlerli, and C. Studerus, *J. High Energy Phys.* 06 (2010) 094.
- [60] T. Gehrmann and D. Kara, *J. High Energy Phys.* 09 (2014) 174.
- [61] A. Chakraborty, T. Huber, R. N. Lee, A. von Manteuffel, R. M. Schabinger, A. V. Smirnov, V. A. Smirnov, and M. Steinhauser, *Phys. Rev. D* **106**, 074009 (2022).
- [62] R. N. Lee, A. von Manteuffel, R. M. Schabinger, A. V. Smirnov, V. A. Smirnov, and M. Steinhauser, *Phys. Rev. Lett.* **128**, 212002 (2022).
- [63] G. P. Korchemsky and G. Marchesini, *Phys. Lett. B* **313**, 433 (1993).
- [64] A. V. Belitsky, *Phys. Lett. B* **442**, 307 (1998).
- [65] Y. Li, A. von Manteuffel, R. M. Schabinger, and H. X. Zhu, *Phys. Rev. D* **91**, 036008 (2015).
- [66] C. Duhr, B. Mistlberger, and G. Vita, *J. High Energy Phys.* 09 (2022) 155.

- [67] C. W. Bauer and A. V. Manohar, *Phys. Rev. D* **70**, 034024 (2004).
- [68] S. W. Bosch, B. O. Lange, M. Neubert, and G. Paz, *Nucl. Phys.* **B699**, 335 (2004).
- [69] T. Becher and M. Neubert, *Phys. Lett. B* **637**, 251 (2006).
- [70] T. Becher and M. D. Schwartz, *J. High Energy Phys.* **02** (2010) 040.
- [71] R. Brüser, Z. L. Liu, and M. Stahlhofen, *Phys. Rev. Lett.* **121**, 072003 (2018).
- [72] P. Banerjee, P. K. Dhani, and V. Ravindran, *Phys. Rev. D* **98**, 094016 (2018).
- [73] T. Becher and G. Bell, *Phys. Lett. B* **695**, 252 (2011).
- [74] T. Inami, T. Kubota, and Y. Okada, *Z. Phys. C* **18**, 69 (1983).
- [75] A. Djouadi, J. Kalinowski, and P. M. Zerwas, *Z. Phys. C* **54**, 255 (1992).
- [76] K. G. Chetyrkin, B. A. Kniehl, and M. Steinhauser, *Phys. Rev. Lett.* **79**, 353 (1997).
- [77] P. A. Baikov, K. G. Chetyrkin, and J. H. Kühn, *Phys. Rev. Lett.* **118**, 082002 (2017).
- [78] T. Ahmed, M. Mahakhud, P. Mathews, N. Rana, and V. Ravindran, *J. High Energy Phys.* **08** (2014) 075.
- [79] S. Fleming, A. H. Hoang, S. Mantry, and I. W. Stewart, *Phys. Rev. D* **77**, 114003 (2008).
- [80] R. Kelley, M. D. Schwartz, R. M. Schabinger, and H. X. Zhu, *Phys. Rev. D* **84**, 045022 (2011).
- [81] T. Becher, M. Neubert, and B. D. Pecjak, *J. High Energy Phys.* **01** (2007) 076.
- [82] S. Catani, M. L. Mangano, P. Nason, and L. Trentadue, *Nucl. Phys.* **B478**, 273 (1996).
- [83] M. Tanabashi *et al.* (Particle Data Group), *Phys. Rev. D* **98**, 030001 (2018).
- [84] D. Baranowski, M. Delto, K. Melnikov, and C.-Y. Wang, *Phys. Rev. D* **106**, 014004 (2022).
- [85] W. Chen, F. Feng, Y. Jia, and X. Liu, *J. High Energy Phys.* **22** (2020) 094.
- [86] I. Moult, I. W. Stewart, G. Vita, and H. X. Zhu, *J. High Energy Phys.* **08** (2018) 013.
- [87] M. Beneke, M. Garny, S. Jaskiewicz, J. Strohm, R. Szafron, L. Vernazza, and J. Wang, *J. High Energy Phys.* **07** (2022) 144.
- [88] T. Becher and M. Neubert, *Phys. Rev. Lett.* **97**, 082001 (2006).
- [89] L. G. Almeida, S. D. Ellis, C. Lee, G. Sterman, I. Sung, and J. R. Walsh, *J. High Energy Phys.* **04** (2014) 174.
- [90] D. Bertolini, M. P. Solon, and J. R. Walsh, *Phys. Rev. D* **95**, 054024 (2017).
- [91] W. Chen, F. Feng, Y. Jia, and X. Liu, *J. High Energy Phys.* **12** (2022) 094.
- [92] D. Baranowski, M. Delto, K. Melnikov, and C.-Y. Wang, *J. High Energy Phys.* **02** (2022) 081.
- [93] G. F. Sterman, *AIP Conf. Proc.* **74**, 22 (1981).
- [94] J. G. M. Gatheral, *Phys. Lett.* **133B**, 90 (1983).
- [95] J. Frenkel and J. C. Taylor, *Nucl. Phys.* **B246**, 231 (1984).
- [96] R. V. Harlander and W. B. Kilgore, *Phys. Rev. D* **68**, 013001 (2003).
- [97] S. Moch, B. Ruijl, T. Ueda, J. A. M. Vermaseren, and A. Vogt, *Phys. Lett. B* **782**, 627 (2018).